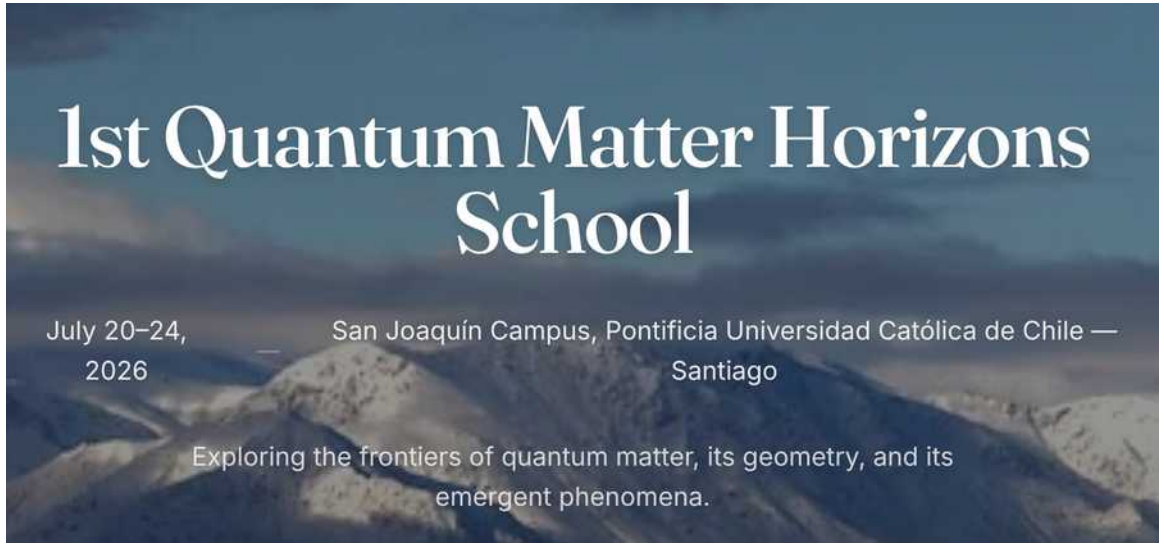

All the material from these lectures will be here:

A primer on Topological Matter

Luis E. F. Foà Torres
Departamento de Física, FCFM, Universidad de Chile

UNC Universidad Nacional de Córdoba

1613 - 2013 400 AÑOS

UERJ Universidade do Estado do Rio de Janeiro

ICTP The Abdus Salam International Centre for Theoretical Physics

cea GRENOBLE

Alexander von Humboldt Stiftung/Foundation

CONICET

UNC Universidad Nacional de Córdoba

Universidad de Chile

quantum transport

2D materials

nanostructures

driven systems

topological insulators

light-matter interaction

quantum materials

many-body interactions and decoherence

electron-phonon interaction

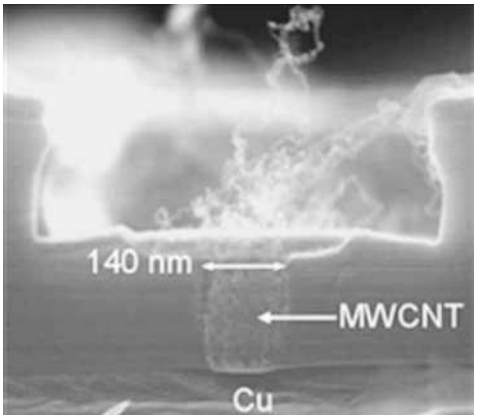

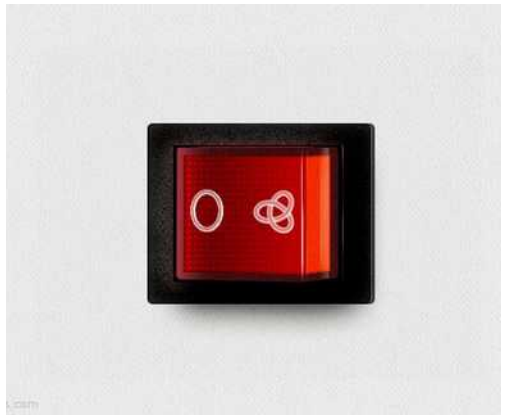

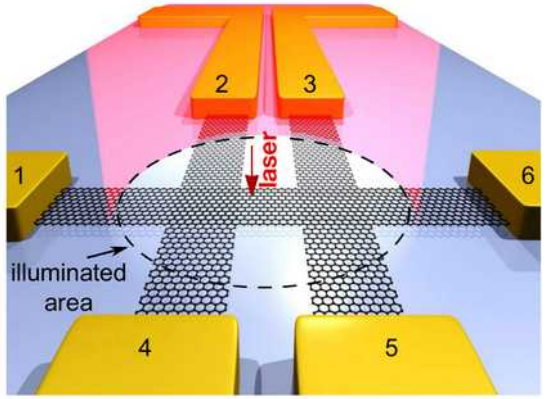

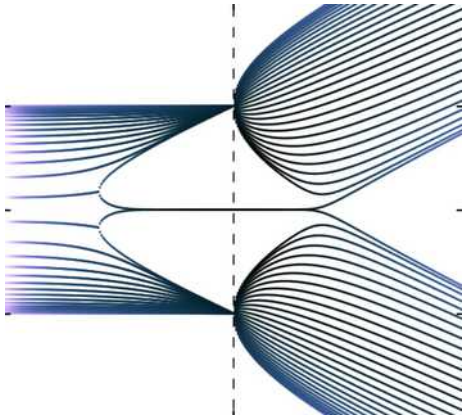

Recently used
Not recently used

https://scimeter.org/

van der Waals he
optoelect
atomistic simulations
tight-bindin
density of states
hone
metallic electrodes
spin
current fluctuations
tunable
electr
charge carriers
surface states
inte
spin current
multi-terminal
quant
graphene ribbons
gate voltage
Landauer
Fano resonance
topolo
zigzag edges
optoelectronic
carbon-
nanodevices
topolog
graphene nanoribbon
laser
Floquet
gate
valley
edge states
pumping
graphene
bilayer graphene
Floquet topological
Dirac point
quasienergy
non-Hermitian
driving frequency
optical phonons
persistent current
topological phases
multilayer graphene
quantum pump
applied voltage
quantum dot coupled
phonon-assisted
gain and loss
phase fluctuations
nonequilibrium Green's function
double barrier
graphene-based
Fock space
quantum dot
phonons
level spacing
Chern number
two-terminal
low bias
Haldane
electrodes
edge states
excitation
topologically protected
scattering theory

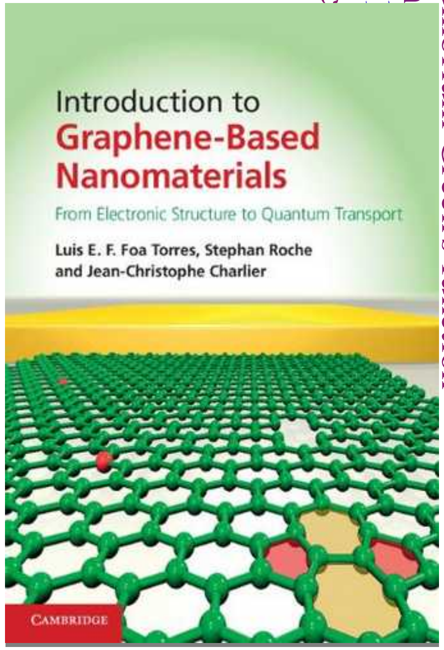

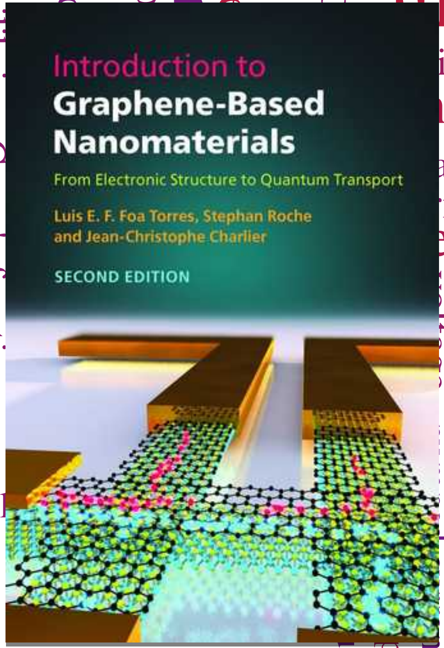

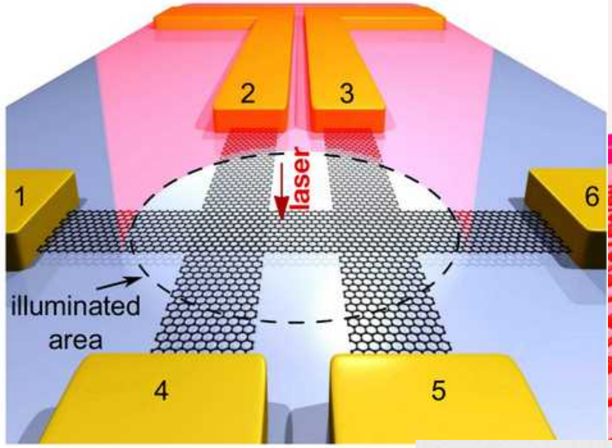

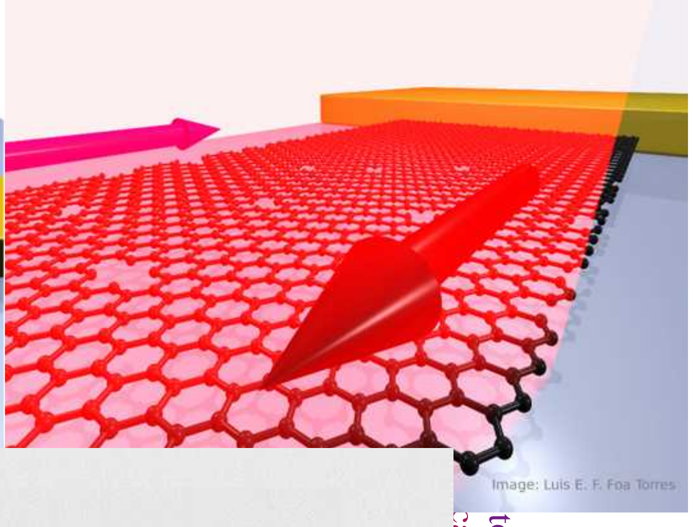

Recently used
Not recently used

https://scimeter.org/

LETTERS
https://doi.org/10.1038/s41567-019-0698-y
nature physics

Light-induced anomalous Hall effect in graphene

J. W. McIver[1,3*], B. Schulte[1,3], F.-U. Stein[1,3], T. Matsuyama[1], G. Jotzu[1], G. Meier[1] and A. Cavalleri[1,2*]

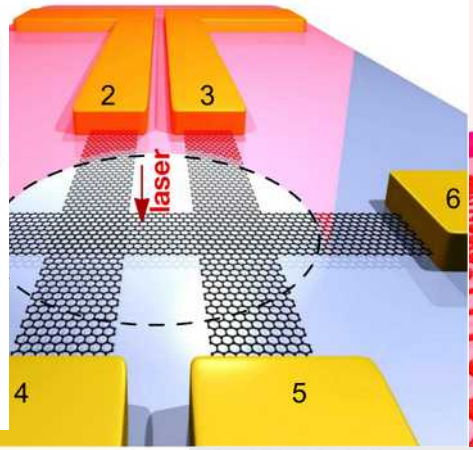

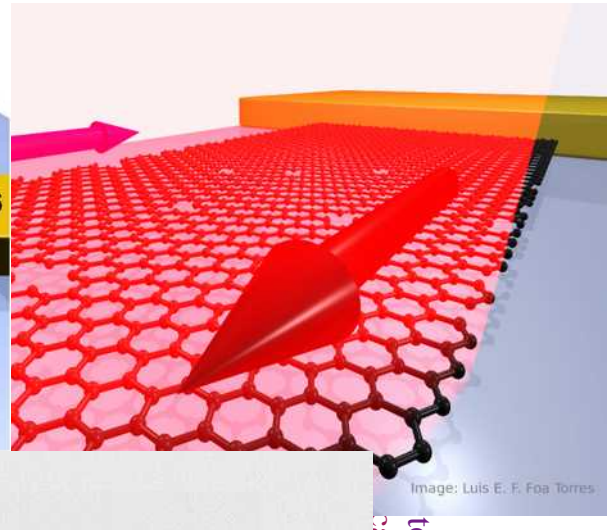

nature physics

Article
https://doi.org/10.1038/s41567-025-02889-7

Observation of Floquet states in graphene

Received: 30 September 2024
Accepted: 21 March 2025
Published online: 6 May 2025
Check for updates

Marco Merboldt[1,9], Michael Schüler[2,3,9], David Schmitt[1], Jan Philipp Bange[1], Wiebke Bennecke[1], Karun Gadge[4], Klaus Pierz[5], Hans Werner Schumacher[5], Davood Momeni[5], Daniel Steil[1], Salvatore R. Manmana[4], Michael A. Sentef[6,7] ✉, Marcel Reutzel[1] ✉ & Stefan Mathias[1,8] ✉

nature physics

Article
https://doi.org/10.1038/s41567-025-02888-8

Observation of Floquet–Bloch states in monolayer graphene

Received: 30 September 2024
Accepted: 21 March 2025
Published online: 01 May 2025
Check for updates

Dongsung Choi[1,8], Masataka Mogi[2,3,8], Umberto De Giovannini[4,5], Doron Azoury[2], Baiqing Lv[2,6], Yifan Su[2], Hannes Hübener[4], Angel Rubio[4,7] & Nuh Gedik[2] ✉

Floquet engineering enables the manipulation of quantum phases of

topologica
aphene nanoribbo
ine
gap
Floquet
laser
gate
valley
edge states
i arcs
pumping
graphene
bilayer graphene
Floquet topological
Dirac point
quasienergy
non-Hermitian
driving frequency
optical phonons
persistent current
topological phases
multilayer graphene
quantum dot coupled
applied voltage
quantum pump
graphene-based
Fock space
quantum dot
phonons
level spacing
Chern number
two-terminal
low bias
phonon-assisted
gain and loss
phase fluctuations
on transport
y-Perot
ge and spin
Haldane
erahertz
electrodes
lators
edge states
pexcitation
ectron system
bes
topologically protected
cattering theory
band structure
d

NANO LETTERS

pubs.acs.org/NanoLett Letter

Engineering Floquet Moiré Patterns for Scalable Photocurrents

Hernán L. Calvo, Luis E. F. Foa Torres, and Matias Berdakin*

Cite This: *Nano Lett.* 2025, 25, 1630−1636 Read Online

ACCESS | Metrics & More | Article Recommendations | Supporting Information

ABSTRACT: While intense laser irradiation and moiré engineering have independently proven powerful for tuning material properties on demand in condensed matter physics, their combination remains unexplored. Here we exploit tilted laser illumination to create spatially modulated light−matter interactions, leading to two striking phenomena in graphene. First, using two lasers tilted along the same axis, we create a quasi-1D supercell hosting a network of Floquet topological states that generate controllable and scalable photocurrents spanning the entire irradiated region. Second, by tilting lasers along orthogonal axes, we establish a 2D polarization moiré pattern giving rise to closed orbital propagation of Floquet states, reminiscent

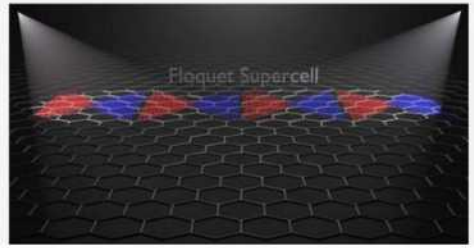

NANO LETTERS

pubs.acs.org/NanoLett Letter

Laser-Induced Spin Precession in Topological Insulator Devices

Esteban A. Rodríguez-Mena, Matías Berdakin,* and Luis E. F. Foa Torres*

Cite This: https://doi.org/10.1021/acs.nanolett.5c03586 Read Online

ACCESS | Metrics & More | Article Recommendations | Supporting Information

ABSTRACT: Controlling spin currents in topological insulators (TIs) is crucial for spintronics but challenged by the robustness of their chiral edge states, which impedes the spin manipulation required for devices such as spin-field effect transistors (SFETs). We theoretically demonstrate that this challenge can be overcome by synergistically applying circularly polarized light and gate-tunable Rashba spin−orbit coupling (rSOC) to a 2D TI. Laser irradiation provides access to Floquet sidebands where rSOC induces controllable spin precession, leading to the generation of one-way, switchable spin-polarized photocurrents, a non-equilibrium effect forbidden in TIs under time-reversal symmetric (equilibrium) conditions. This mechanism effectively realizes SFET functionality within a driven TI, specifically operating within a distinct Floquet replica, offering a new paradigm for light-based control in topological spintronics.

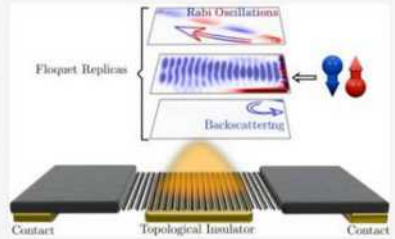

KEYWORDS: *spin photocurrents, topological insulators, two-dimensional materials, spin−orbit coupling*

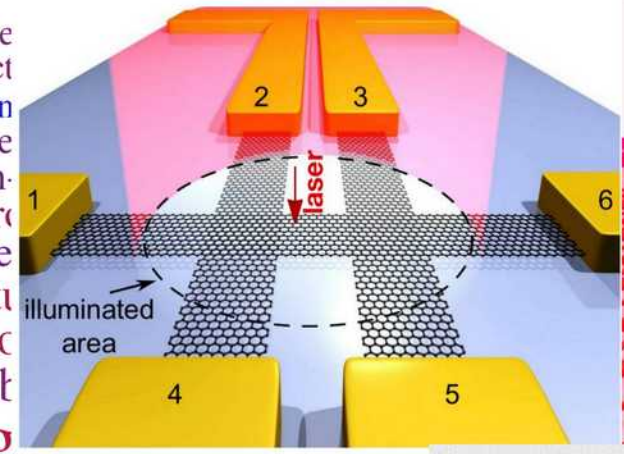

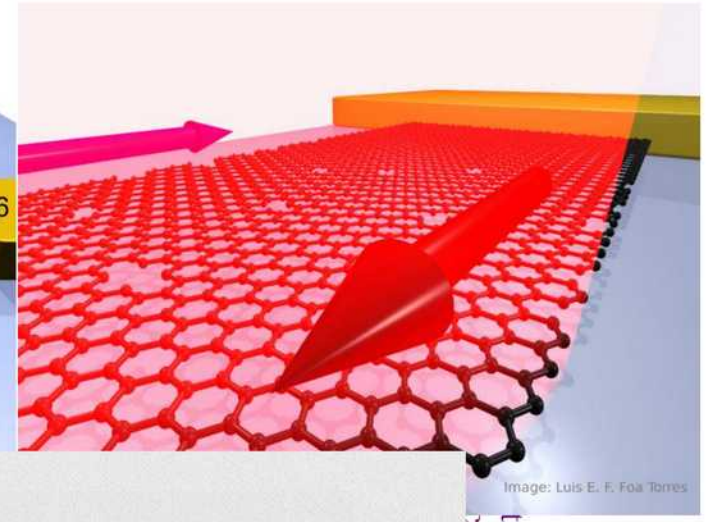

Image: Luis E. F. Foa Torres

nature communications

Article https://doi.org/10.1038/s41467-025-57335-2

Signatures of Floquet electronic steady states in graphene under continuous-wave mid-infrared irradiation

Received: 14 February 2024

Accepted: 19 February 2025

Published online: 28 February 2025

Check for updates

Yijing Liu[1,9], Christopher Yang[2,9], Gabriel Gaertner[3], John Huckabee[3], Alexey V. Suslov[4], Gil Refael[2], Frederik Nathan[5], Cyprian Lewandowski[4,6], Luis E. F. Foa Torres[7], Iliya Esin[2,8] ✉, Paola Barbara[1] ✉ & Nikolai G. Kalugin[3] ✉

Light-induced phenomena in materials can exhibit exotic behavior that extends beyond equilibrium properties, offering new avenues for under-

Many (unexpected) experimental confirmations!

van der Waals heterostructures

atomistic

Precedent of the “non-Hermitian skin effect”

PHYSICAL REVIEW B **97**, 121401(R) (2018)

Rapid Communications

Non-Hermitian robust edge states in one dimension: Anomalous localization and eigenspace condensation at exceptional points

V. M. Martinez Alvarez,[1] J. E. Barrios Vargas,[2] and L. E. F. Foa Torres[2,*]

[1]*Departamento de Física, Laboratório de Física Teórica e Computacional, Universidade Federal de Pernambuco, Recife 50670-901, Pernambuco, Brazil*

[2]*Departamento de Física, Facultad de Ciencias Físicas y Matemáticas, Universidad de Chile, Santiago 837.0415, Chile*

(Received 25 August 2017; revised manuscript received 17 February 2018; published 7 March 2018)

Capital to topological insulators, the bulk-boundary correspondence ties a topological invariant computed from the bulk (extended) states with those at the boundary, which are hence robust to disorder. Here we put forward a different ordering unique to non-Hermitian lattices whereby a pristine system becomes devoid of extended states, a property which turns out to be robust to disorder. This is enabled by a peculiar type of non-Hermitian degeneracy where a macroscopic fraction of the states coalesce at a single point with a geometrical multiplicity of 1.

DOI: 10.1103/PhysRevB.97.121401

Víctor Manuel Martínez Álvarez (UFPe Brazil)

José Eduardo Barrios Vargas (U Chile)

- Quantum walk with photons
  L. Xiao et al. Nature Physics **16**, 761 (2020)
- Circuits
  T. Hofmann et al. Phys. Rev. Research **2**, 023265 (2020)
- Acoustic systems and metamaterials
  Li Zhang et al. Nature Communications **12**, 6297 (2021)
  M. Brandenbourger et al. Nat. Comms. **10**, 4608 (2019)
- Active matter
  L. S. Palacios et al. Nat. Comms. **12**, 4691 (2021)
- Ultracold matter
  Q. Liang et al. arxiv:2201.09478

bilayer graphene
Floquet topological
Dirac point
non-Hermitian
driving frequency
optical phonons
persistent current
topological phases
multilayer graphene
quantum dot coupled
applied voltage
quantum pump
graphene-based
double barrier
voltage pumped current
antum transport gapless
terface states spin pumping
ation
yers
lock space
phonons
quantum dot
level spacing
Chern number
quasienergy
two-terminal
low bias
phonon-assisted
gain and loss
phase fluctuations
ron transport
ry-Perot
ge and spin
Haldane
erahertz
electrodes
lators
edge states
excitation
ectron system
bes

Recently used
Not recently used

https://scimeter.org/

Organization of these lectures

Brief motivation: What's the hype about topological matter?

Topology in one dimension: The SSH model

Graphene's bandstructure

The many faces of the Quantum Hall Effect

From Haldane's model to Topological Insulators

New directions

All the material from these lectures will be here:

Quantum materials: where the many paths meet

Quantum effects are everywhere
but in some materials they become evident
at a wider range of energy and length scales.

Quantum materials include superconductors,
graphene, **topological insulators**, Weyl semimetals, quantum spin liquids,
and more.

Sources of the underlying properties include:
reduced dimensionality and **interactions**.

Quantum Hall effects

Macroscopic quantum phenomena

Quantum Hall effects

artificial systems
under
extreme conditions

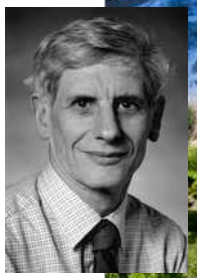

materials
and
applications

Quantum Hall effects

PHYSICAL REVIEW LETTERS **122,** 200001 (2019)

Essay: Quantum Hall Effect and the New International System of Units

Klaus von Klitzing
Max Planck Institut für Festkörperforschung, Heisenbergstraße 1, D-70569 Stuttgart, Germany

(Received 18 March 2019; published 20 May 2019)

On 20 May 2019 the International System of Units will switch over to a new, globally accepted set of definitions based on constants of nature. The quantum Hall effect, discovered 39 years ago, plays an essential role in this development and will now contribute to a new definition of the kilogram. Ironically, the title of publication in *Physical Review Letters* that introduced the quantum Hall effect is, in hindsight, inaccurate in view of the revised units [K. von Klitzing, G. Dorda, and M. Pepper, New Method for High-Accuracy Determination of the Fine-Structure Constant Based on Quantized Hall Resistance, Phys. Rev. Lett. **45**, 494 (1980)].

DOI: 10.1103/PhysRevLett.122.200001

materials
and
applications

Quantum Hall effects

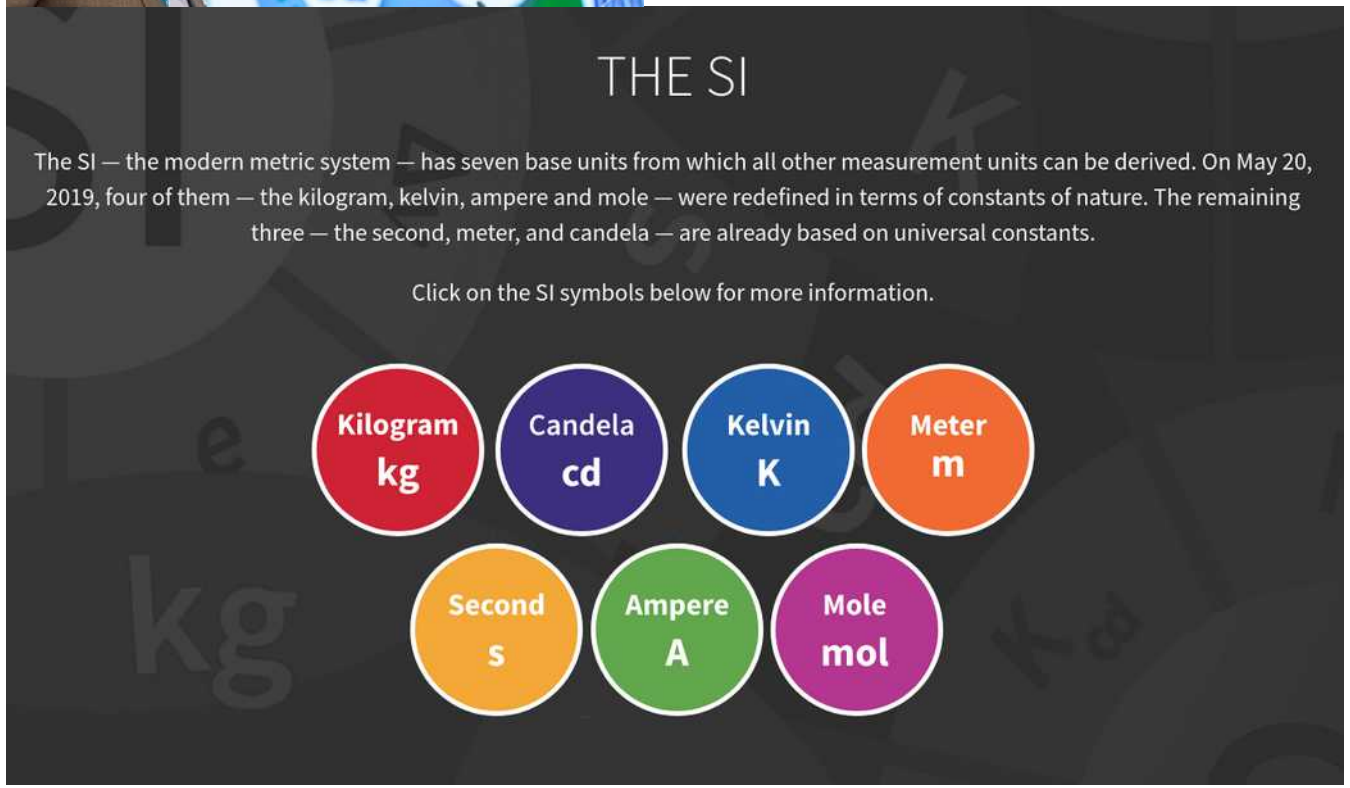

https://www.nist.gov/si-redefinition

materials
and
applications

Against all odds, topological properties turned out to be ubiquitous

Quantum Hall effects

[Submitted on 20 May 2021]

arXiv:2105.09954 [cond-mat.mtrl-sci]

All Topological Bands of All Stoichiometric Materials

Maia G. Vergniory,[1,2,*] Benjamin J. Wieder,[3,4,5,*] Luis Elcoro,[6] Stuart S. P. Parkin,[7] Claudia Felser,[8] B. Andrei Bernevig,[5] and Nicolas Regnault[5,9,†]

38,298 unique materials (nonmagnetic)

52.65% of all materials are topological at EF

materials
and
applications

Organization of these lectures

Brief motivation: What's the hype about topological matter?

Topology in one dimension: The SSH model

Graphene's bandstructure

The many faces of the Quantum Hall Effect

From Haldane's model to Topological Insulators

New directions

All the material from these lectures will be here:

QUANTUM MATTER HORIZONS SCHOOL · 2026

Lecture 1
Topology in one dimension: the SSH model

From dimerization to protected boundary states

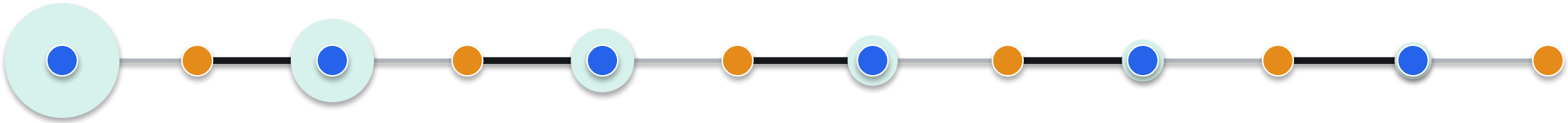

Luis E. F. Foà Torres · Universidad de Chile

foatorres.com · @foatorres

Historical context for the SSH model

Werner Heisenberg and Felix Bloch around 1931

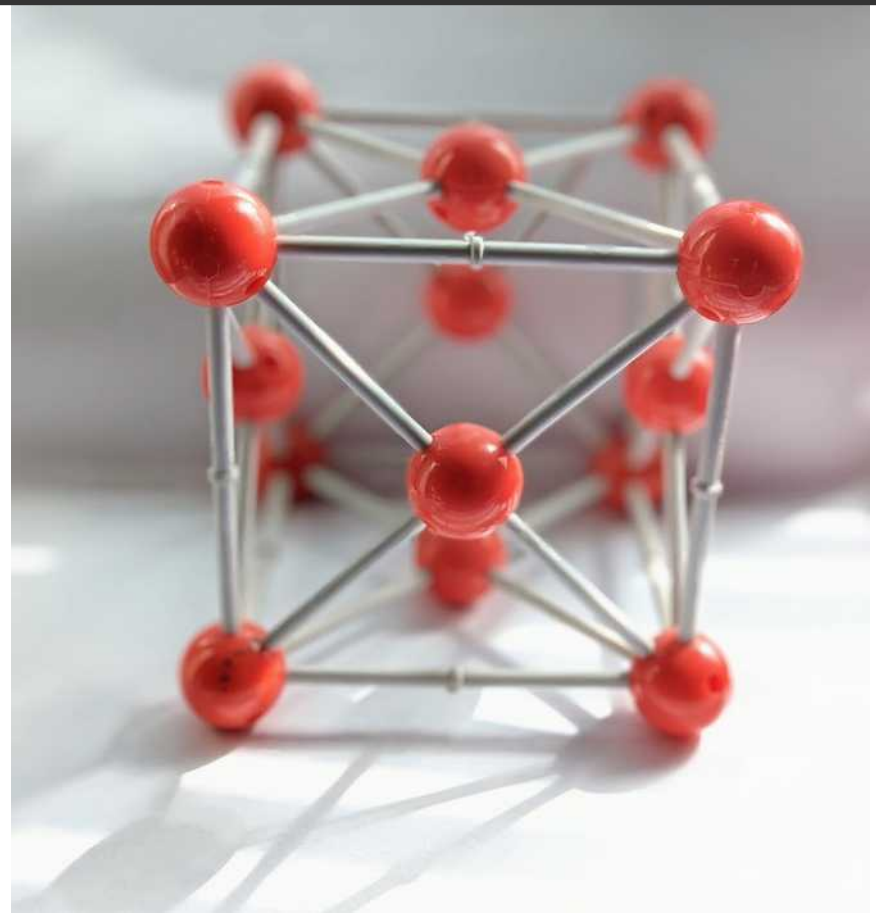

A long history of electron-phonon interaction in solids

ANNALEN DER PHYSIK

5. FOLGE, 1930, BAND 4, HEFT 2

Zur Theorie der elektrischen und thermischen Leitfähigkeit von Metallen

Von R. Peierls

(Mit 1 Figur)

Einleitung

Die Frage nach dem *Mechanismus* der Elektronenbewegung in Metallen ist seit den Untersuchungen von Bloch[1]) als ziemlich abgeschlossen anzusehen. Es wurde dort u. a. gezeigt, daß sich ein Elektron in einem rein periodischen Kraftfeld ungehindert bewegen kann, daß also ein Widerstand immer erst durch die thermische Bewegung des Gitters zustande kommt. Die Verhältnisse liegen ähnlich wie bei der Streuung von Röntgenstrahlen; Houston[2]) und Frenkel[3]) versuchten, die Wechselwirkung zwischen den Elektronen und den Gitterschwingungen genau analog zu der bekannten Beugungstheorie für Röntgenstrahlen zu behandeln. Bloch zeigte jedoch, daß

The Electrical Resistance of Metals.

P. W. Bridgman

Phys. Rev. **17**, 161 – Published 1 February 1921

REVIEWS OF MODERN PHYSICS VOLUME 23, NUMBER 3 JULY, 1951

Electron-Vibration Interactions and Superconductivity

J. BARDEEN*

Bell Telephone Laboratories, Murray Hill, New Jersey

A long history of e-ph interaction in solids: The Peierls' transition

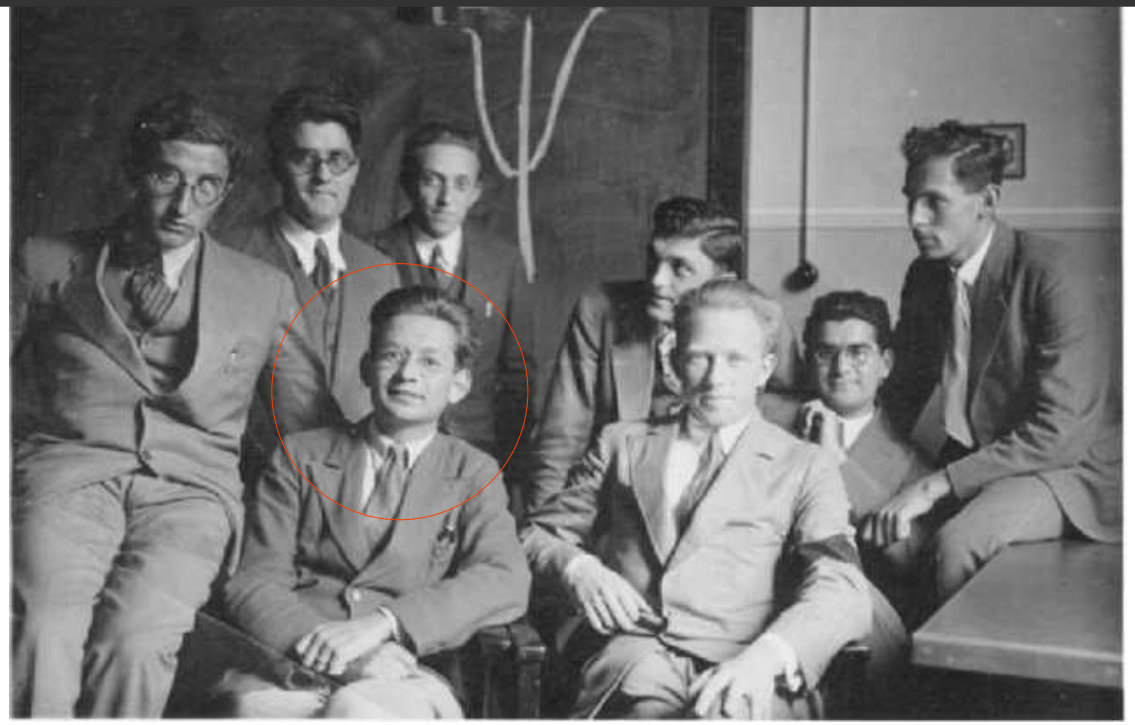

Heisenberg's Institute in Leipzig, 1931. Front row (L-R): George Placzek (sitting on desk), **Rudolf Peierls** and Werner Heisenberg; back row (L-R): Giovanni Gentile Jr., Gian Carlo Wick, Felix Bloch, Viktor Weisskopf and Fritz Sauter.
Copyright: Alessandra Gentile

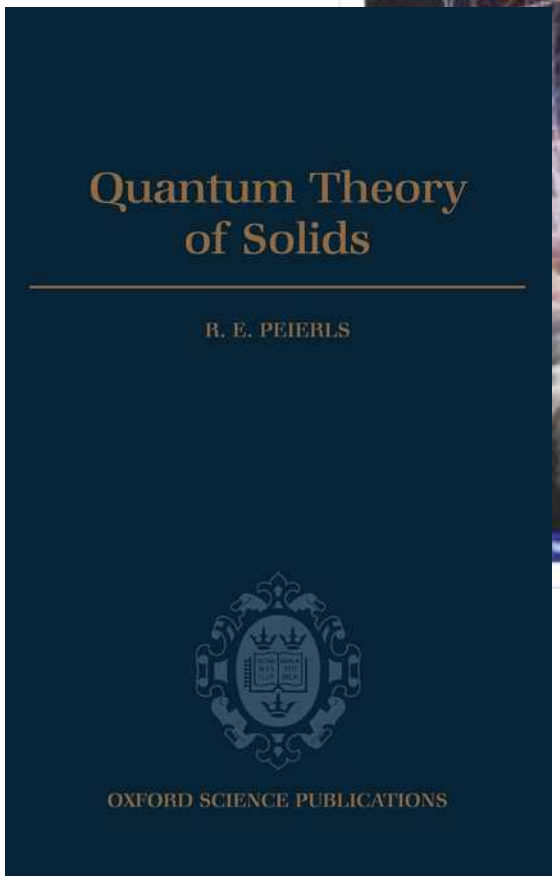

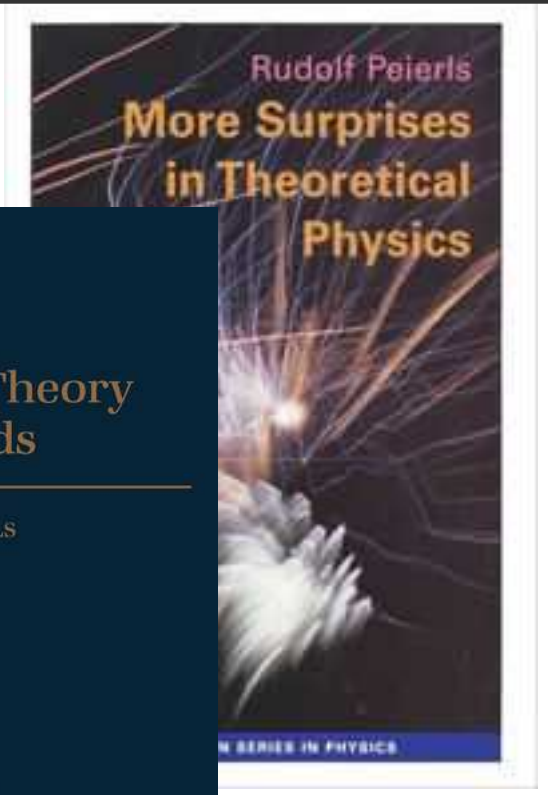

A long history of e-ph interaction in solids: The Peierls' transition

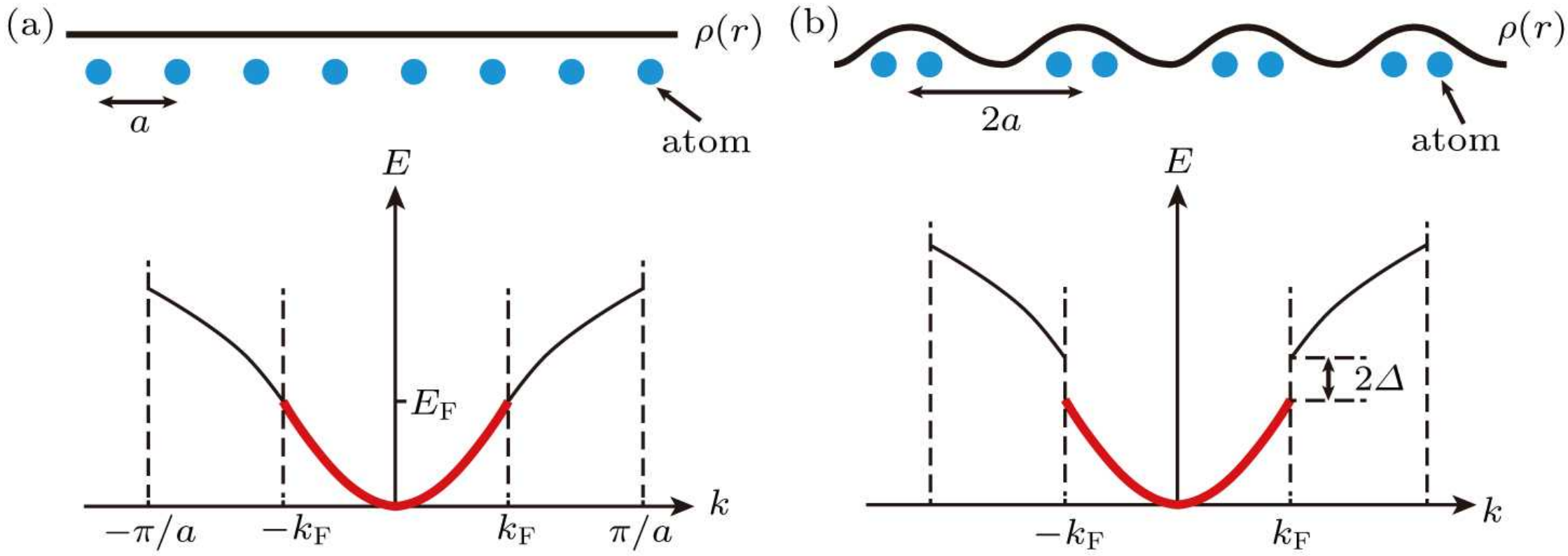

metal

Peierls' insulator

G. Grüner, *The dynamics of charge density waves*, Rev. Mod. Phys. **60**, 1129 (1988)

A long history of e-ph interaction in solids: The Peierls' transition

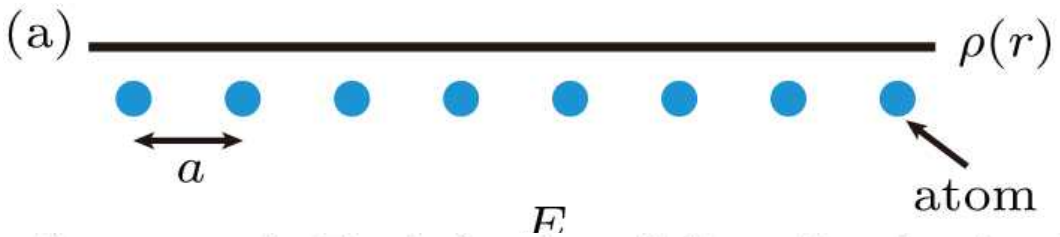

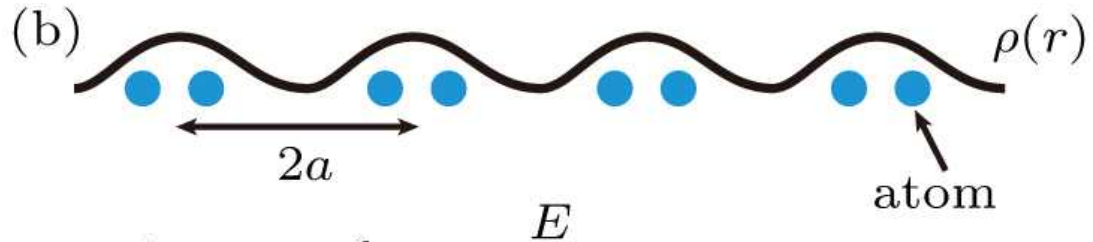

placement δ. The behavior of the reduction in electronic energy for small displacement is therefore as

$$-\delta^2 \log \delta. \qquad (2.3.5)$$

This is interesting because there may be other effects favoring the regular spacing, $\delta = 0$, such as the repulsion between the atomic cores, but these will have an energy varying as δ^2, and therefore the electron energy must dominate for small displacement. This suggests that the periodic chain must always be unstable.

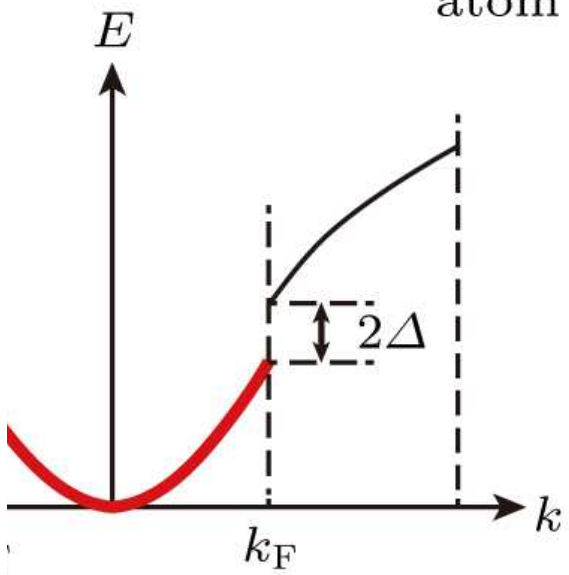

metal

Peierls' insulator

G. Grüner, *The dynamics of charge density waves*, Rev. Mod. Phys. **60**, 1129 (1988)

A long history of e-ph interaction in solids: The Peierls' transition

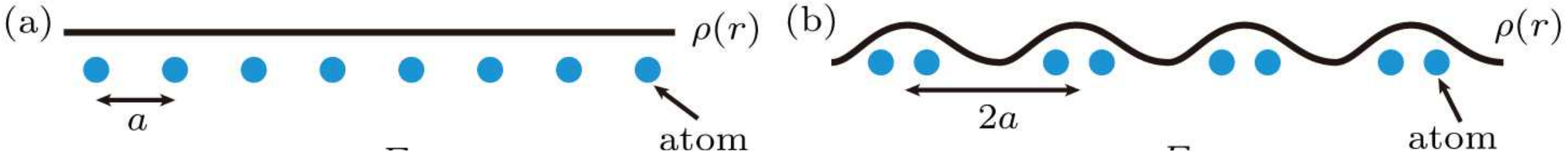

Behavior as a function of temperature, CDWs, critical temperature T_c

G. Grüner, *The dynamics of charge density waves*, Rev. Mod. Phys. **60**, 1129 (1988)

A long history of e-ph interaction in solids: The Peierls' transition

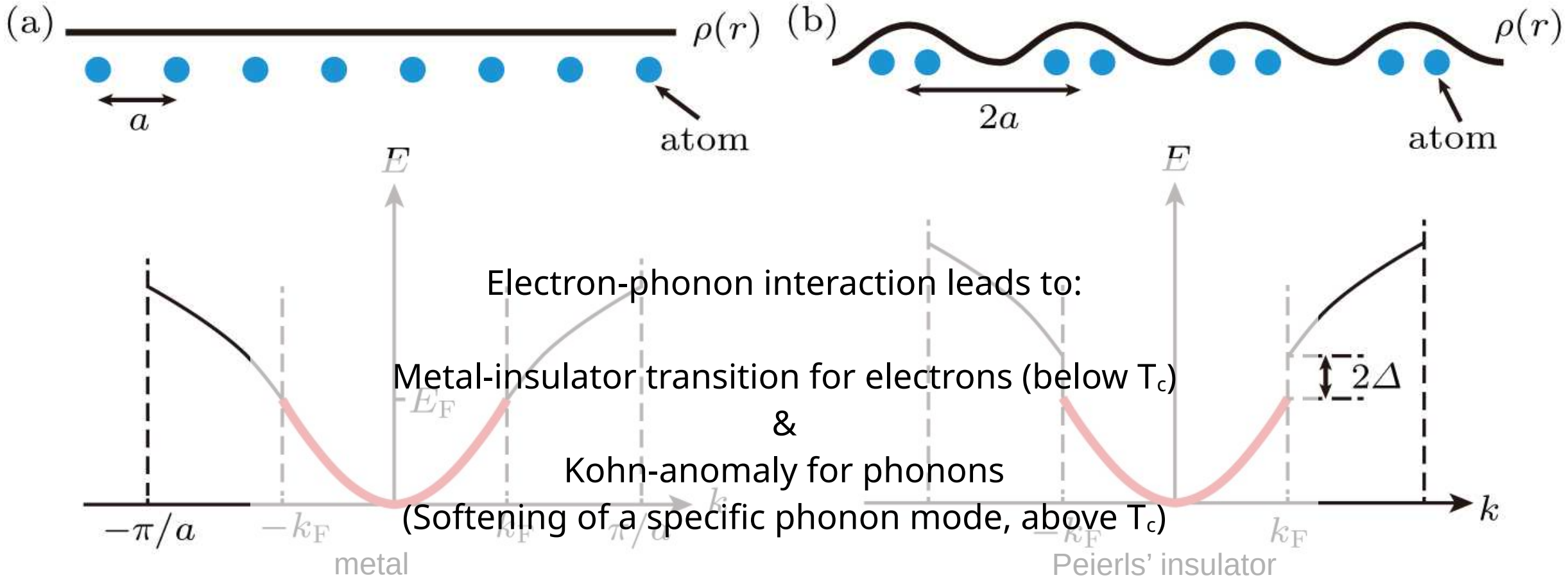

Electron-phonon interaction leads to:

Metal-insulator transition for electrons (below T_c)

&

Kohn-anomaly for phonons

(Softening of a specific phonon mode, above T_c)

G. Grüner, *The dynamics of charge density waves*, Rev. Mod. Phys. **60**, 1129 (1988)

A long history of e-ph interaction in solids: The Peierls' transition

This instability came to me as a complete surprise when I was tidying material for my book (Peierls 1955), and it took me a considerable time to convince myself that the argument was sound. It seemed of only academic significance, however, since there are no strictly one-dimensional systems in nature (and if there were, they would become disordered at any finite temperature; see *Surprises*, sec. 4.1). I therefore did not think it worth publishing the argument, beyond a brief remark in the book, which did not even mention the logarithmic behavior.

In this case the first surprise was in the mathematical result for the one-dimensional case; a second surprise was that this had some connection with reality.

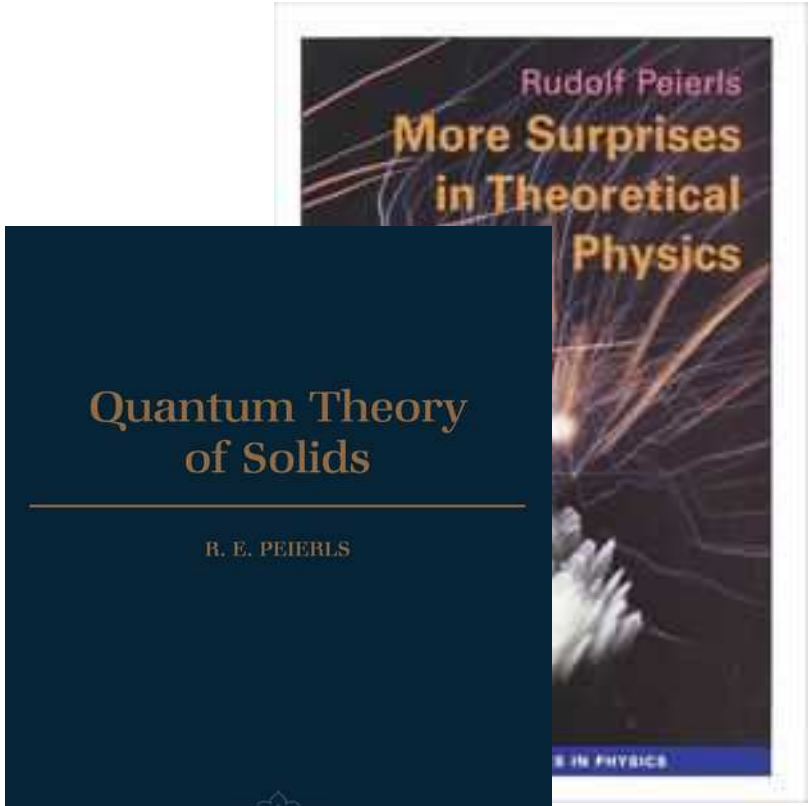

A long history of e-ph interaction in solids: Conducting polymers

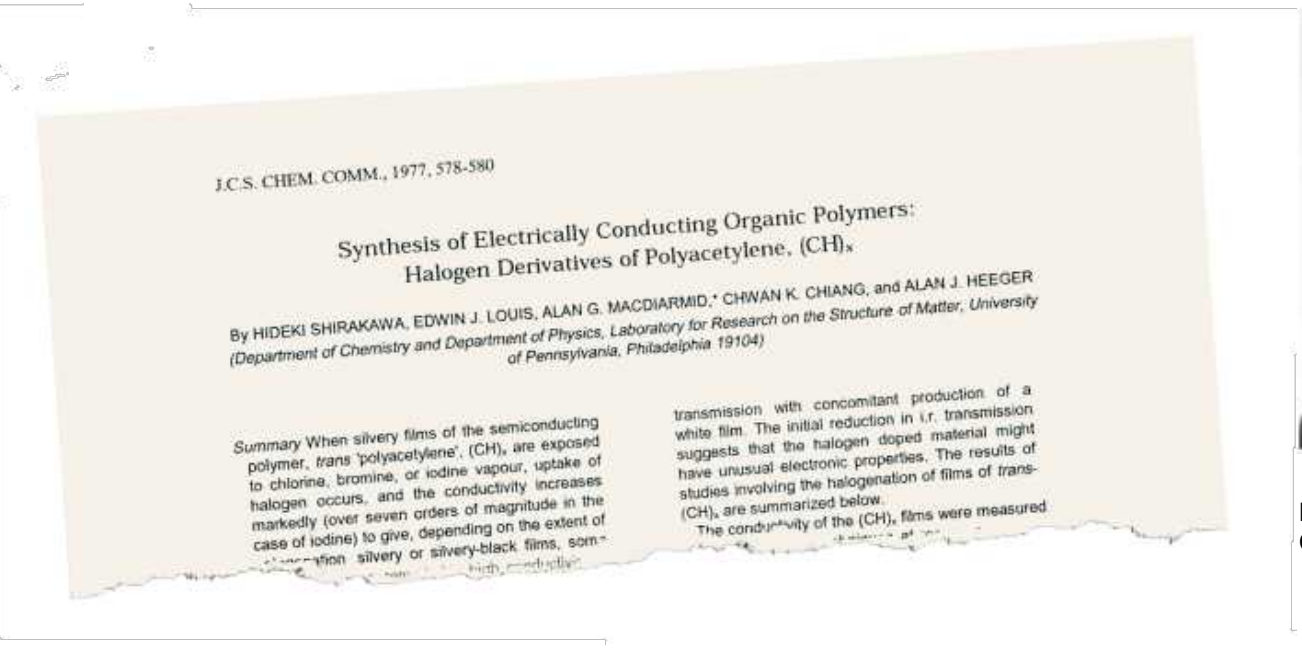

J.C.S. CHEM. COMM., 1977, 578-580

Synthesis of Electrically Conducting Organic Polymers:
Halogen Derivatives of Polyacetylene, $(CH)_x$

By HIDEKI SHIRAKAWA, EDWIN J. LOUIS, ALAN G. MACDIARMID,* CHWAN K. CHIANG, and ALAN J. HEEGER
(Department of Chemistry and Department of Physics, Laboratory for Research on the Structure of Matter, University of Pennsylvania, Philadelphia 19104)

Summary When silvery films of the semiconducting polymer, *trans* 'polyacetylene', $(CH)_x$, are exposed to chlorine, bromine, or iodine vapour, uptake of halogen occurs, and the conductivity increases markedly (over seven orders of magnitude in the case of iodine) to give, depending on the extent of [illegible] silvery or silvery-black films, some [illegible] transmission with concomitant production of a white film. The initial reduction in i.r. transmission suggests that the halogen doped material might have unusual electronic properties. The results of studies involving the halogenation of films of *trans*-$(CH)_x$ are summarized below.

The conductivity of the $(CH)_x$ films were measured

Hideki Shirakawa, Alan MacDiarmid and Alan Heeger, Nobel prize in Chemistry 2000

A long history of e-ph interaction in solids: Conducting polymers

VOLUME 42, NUMBER 25 PHYSICAL REVIEW LETTERS 18 JUNE 1979

Solitons in Polyacetylene

W. P. Su, J. R. Schrieffer, and A. J. Heeger
Department of Physics, University of Pennsylvania, Philadelphia, Pennsylvania 19104
(Received 15 March 1979)

We present a theoretical study of soliton formation in long-chain polyenes, including the energy of formation, length, mass, and activation energy for motion. The results provide an explanation of the mobile neutral defect observed in undoped $(CH)_x$. Since the soliton formation energy is less than that needed to create band excitation, solitons play a fundamental role in the charge-transfer doping mechanism.

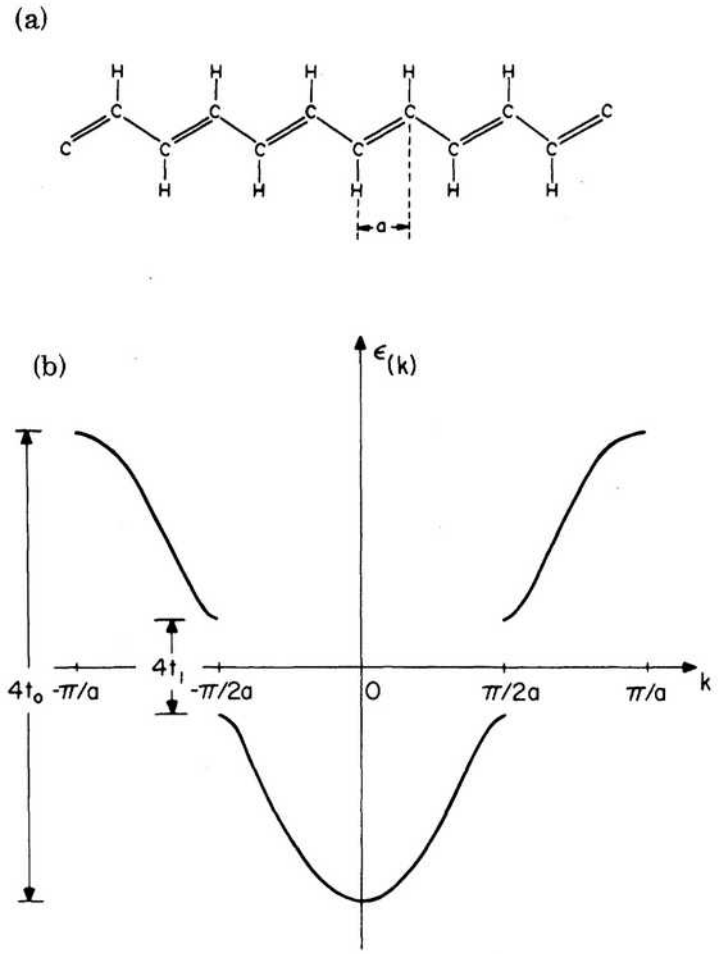

FIG. 1. (a) *Trans* configuration of $(CH)_x$. $a = 1.2$ Å. (b) π-band structure of perfectly dimerized $(CH)_x$.

Two gapped chains. The same insulator?

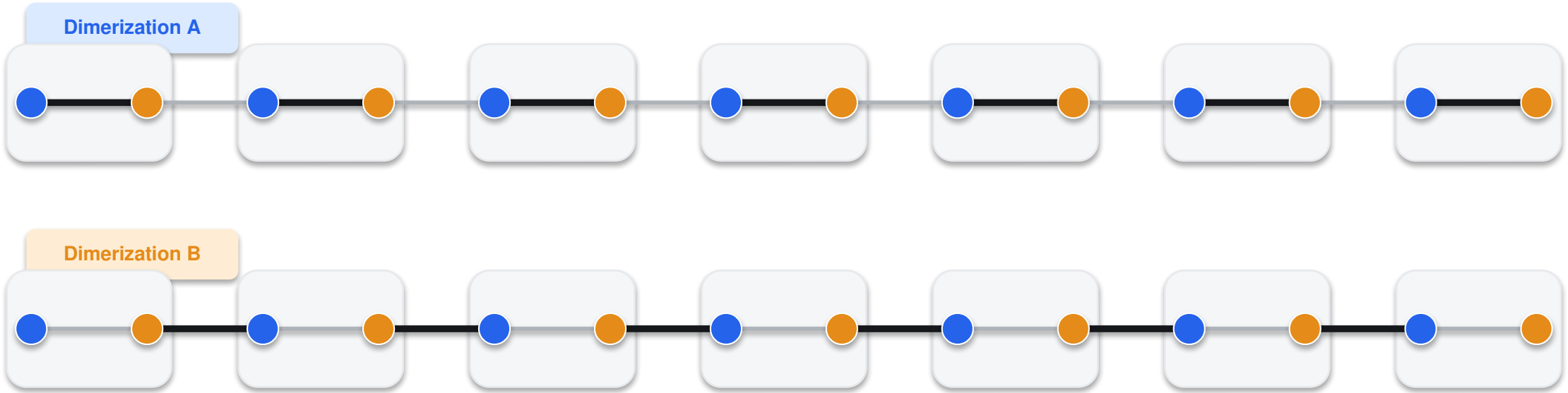

Both have **two sites per cell** · two bands · a finite bulk gap

Can a bulk property distinguish them?

Where the model comes from: polyacetylene

A uniform half-filled chain

metallic in the simplest picture

Peierls distortion

Two degenerate dimerized patterns

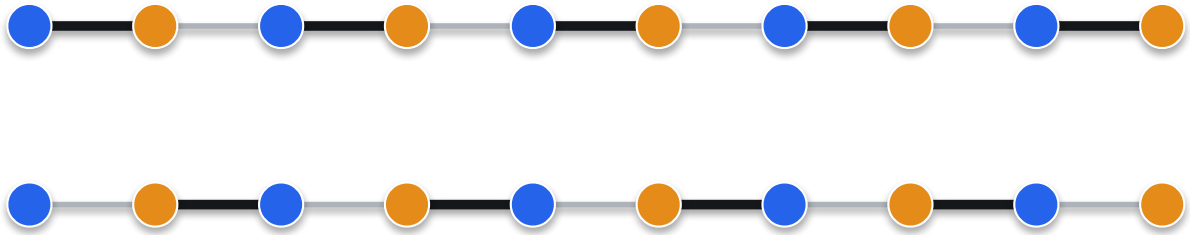

A lattice distortion opens a gap — but it also creates two possible insulating ground states.

W. P. Su, J. R. Schrieffer & A. J. Heeger, Phys. Rev. Lett. 42, 1698 (1979)

The distinction becomes visible at a boundary

Strong bonds at the ends

Weak bonds at the ends

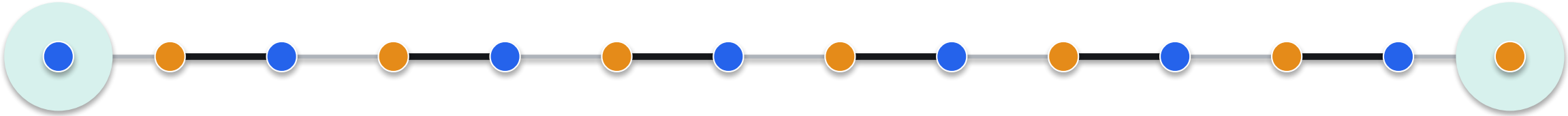

unpaired end degrees of freedom

We now look for a bulk statement that predicts this boundary difference.

The SSH Hamiltonian

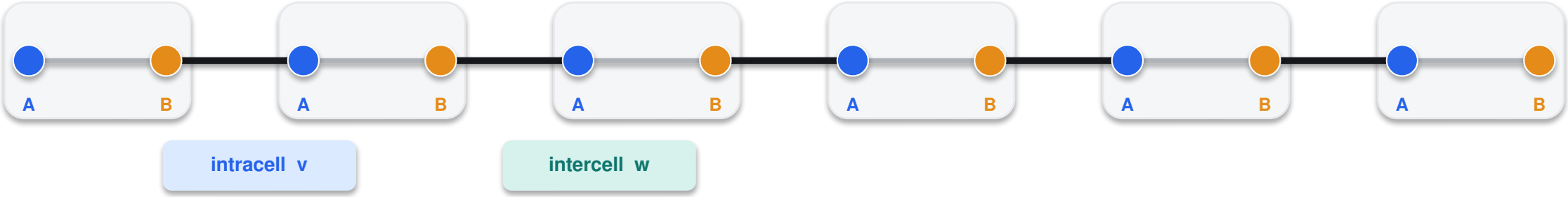

$$\hat{H} = \sum_n \left(v\, a_n^\dagger b_n + w\, a_{n+1}^\dagger b_n + \text{h.c.} \right)$$

- one orbital per site; two sites A and B per unit cell
- spin is suppressed for simplicity
- nearest-neighbor hopping only; take both hoppings to be positive

Two limits you can solve by eye

$w = 0$ **only intracell bonds**

isolated dimers — every site is paired

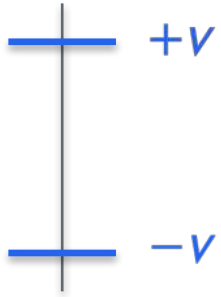

two flat bands at ±v
nothing inside the gap

$v = 0$ **only intercell bonds**

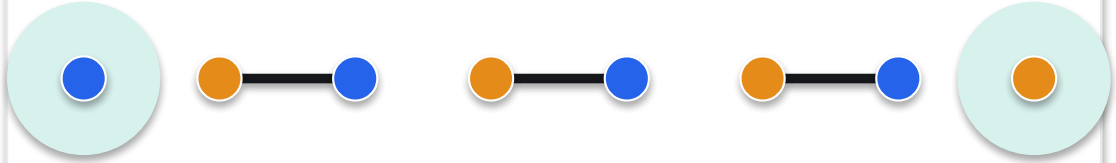

the two end sites decouple completely

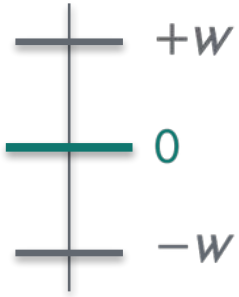

two states pinned exactly
at zero energy — one per end

Away from these limits the bonds compete. Which features survive at general v, w — and why?

From the lattice to momentum space

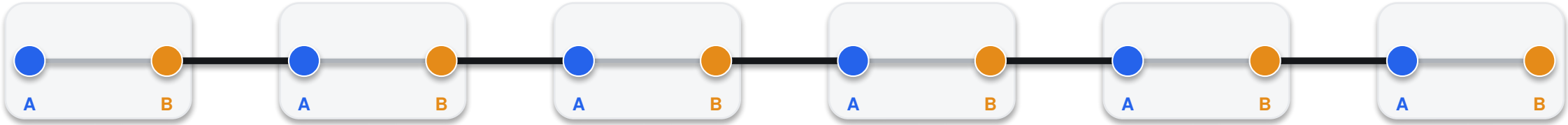

cell n

$$a_n = \frac{1}{\sqrt{N}} \sum_k e^{ikna} a_k$$

$$b_n = \frac{1}{\sqrt{N}} \sum_k e^{ikna} b_k$$

a = unit-cell length · N = number of cells

$$|\psi_k\rangle = \begin{pmatrix} a_k & b_k \end{pmatrix}^{\mathsf{T}}$$

The bulk problem is now a 2 × 2 eigenvalue equation.

A two-band Bloch Hamiltonian

$$H(k)|u_k\rangle = E(k)|u_k\rangle$$

$$H(k) = \begin{pmatrix} 0 & q^*(k) \\ q(k) & 0 \end{pmatrix}$$

$$q(k) = v + we^{ika}$$

all the geometry is
contained in one complex number

The diagonal vanishes because there are no A–A or B–B terms.

The Hamiltonian as a vector

$$H(k) = d_x(k)\sigma_x + d_y(k)\sigma_y$$

$$d_x(k) = v + w\cos(ka)$$

$$d_y(k) = w\sin(ka)$$

$$d_z(k) = 0$$

As momentum changes, the Hamiltonian vector draws a closed path in a plane.

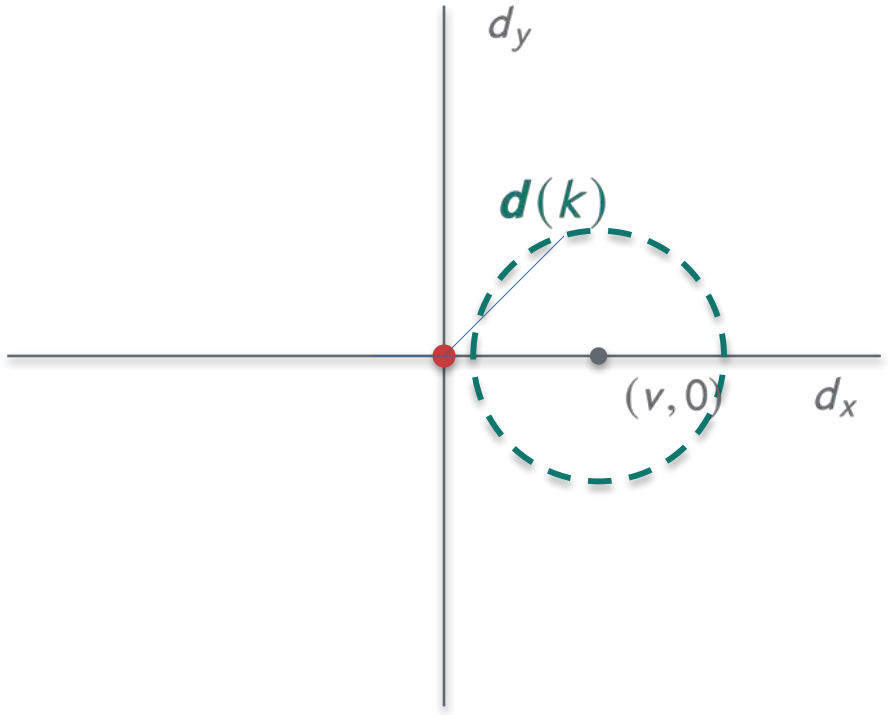

the tip traces the dashed circle once per Brillouin zone

The bands do not yet reveal the distinction

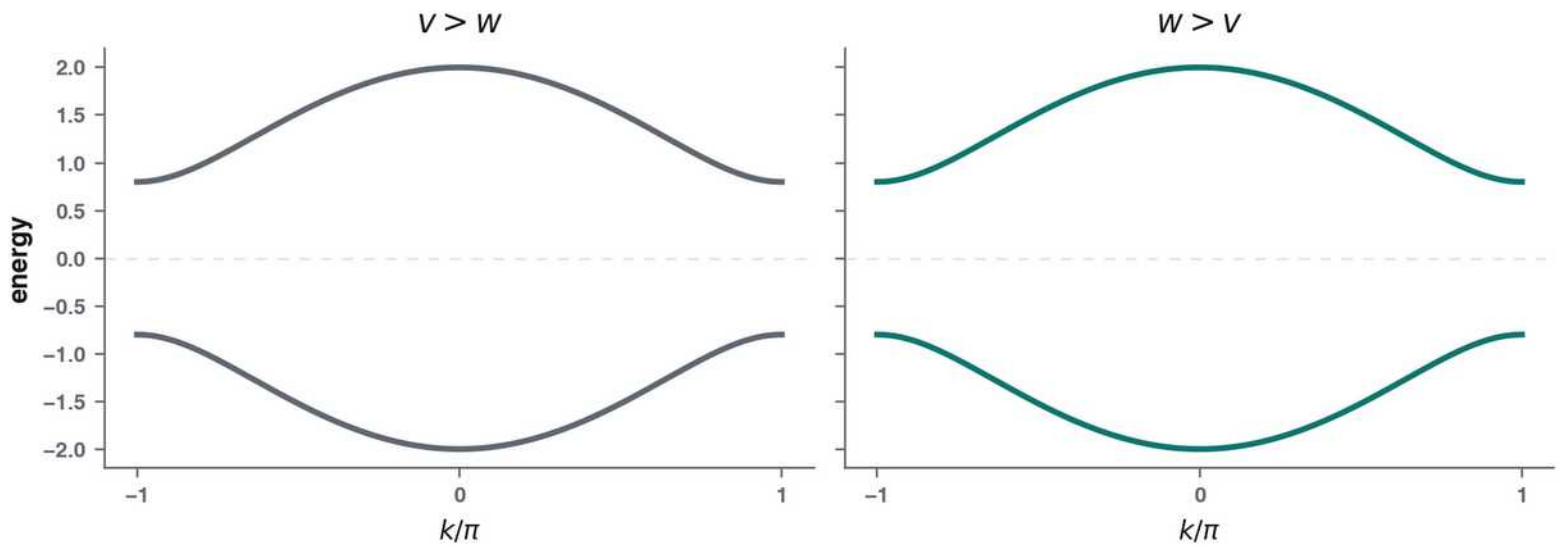

$$E_{\pm}(k) = \pm|q(k)|$$

Both sides have
- two bands
- a symmetric spectrum
- a finite gap

Something besides the eigenvalues is needed.

To move between the two regimes, the gap must close

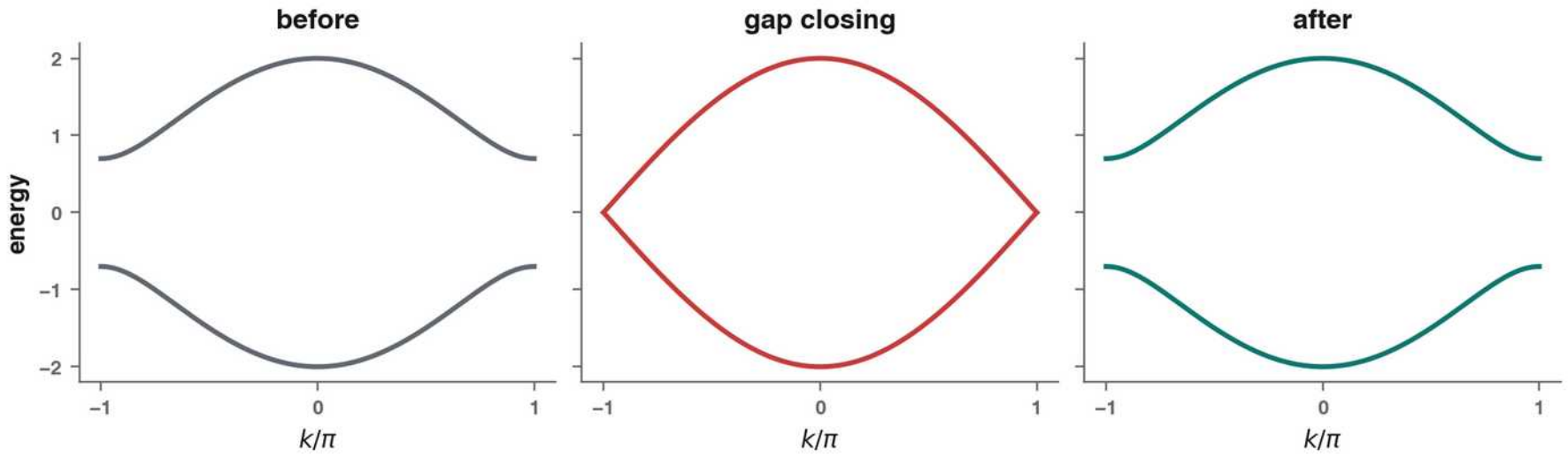

$$\nu = w$$

$$q(\pi/a) = 0$$

$$E_{\pm}(\pi/a) = 0$$

The insulating state is undefined at the transition.

Whatever bulk number distinguishes the two regimes, it can change only at a gap closing.

The protecting constraint: chiral symmetry

hopping connects A only to B

$$\Gamma = \sigma_z$$

$$\Gamma H(k) \Gamma^{-1} = -H(k)$$

Equivalently: $\{\Gamma, H(k)\} = 0$

Chiral symmetry forbids an out-of-plane component: the path of d(k) is pinned to the plane.

What chiral symmetry buys us

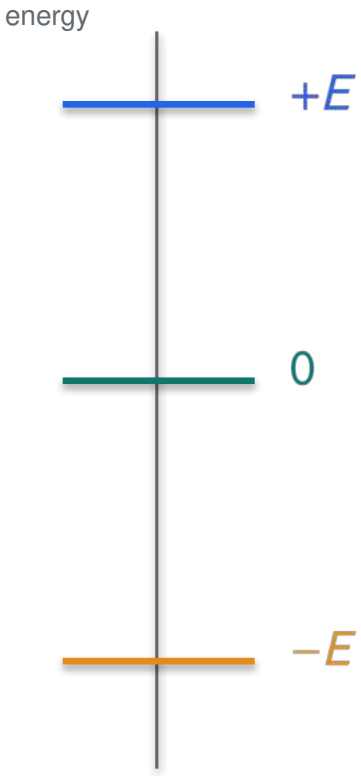

Spectral pairing

$$H|\psi\rangle = E|\psi\rangle$$

$$H\Gamma|\psi\rangle = -E\Gamma|\psi\rangle$$

Where eigenstates live

E ≠ 0 — equal weight on A and B

E = 0 — one sublattice only

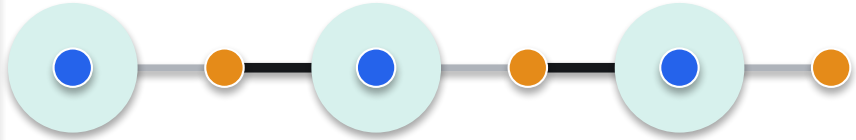

an isolated zero mode can be chosen as a chiral eigenstate — pinned to one sublattice

The Brillouin zone becomes a closed curve

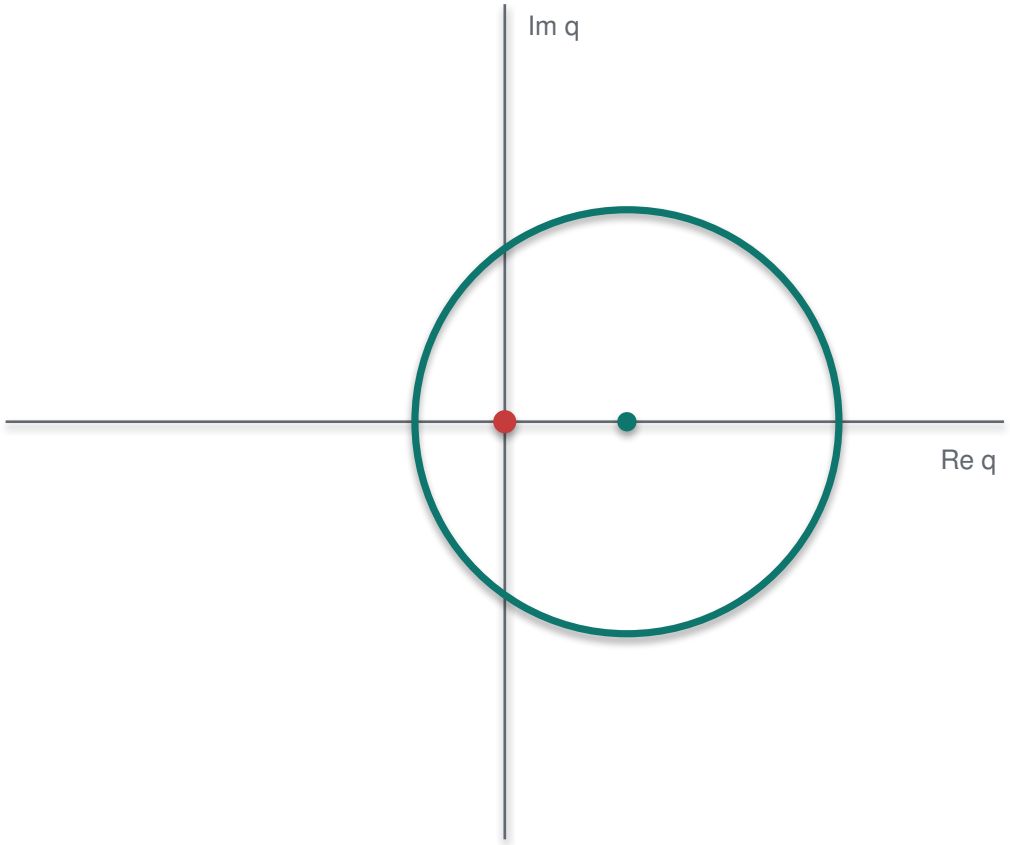

$$q(k) = v + we^{ika}$$

$$q(k) = d_x(k) + i\, d_y(k)$$

the same closed path as the d-vector, read as one complex number

- center: v
- radius: w
- one circuit as k crosses the BZ

The origin is the gap-closing point.

Counting how many times the curve winds

$$q(k) = |q(k)|e^{i\theta(k)}$$

$$\nu = \frac{1}{2\pi}\int_{\mathrm{BZ}} dk\, \partial_k \theta(k)$$

$\nu = 0$ origin outside

$\nu = 1$ origin enclosed

The winding is integer-valued: it cannot drift continuously under a smooth deformation.

J. K. Asbóth, L. Oroszlány & A. Pályi, A Short Course on Topological Insulators, Lect. Notes Phys. 919 (Springer, 2016) · arXiv:1509.02295

Two phases and the transition between them

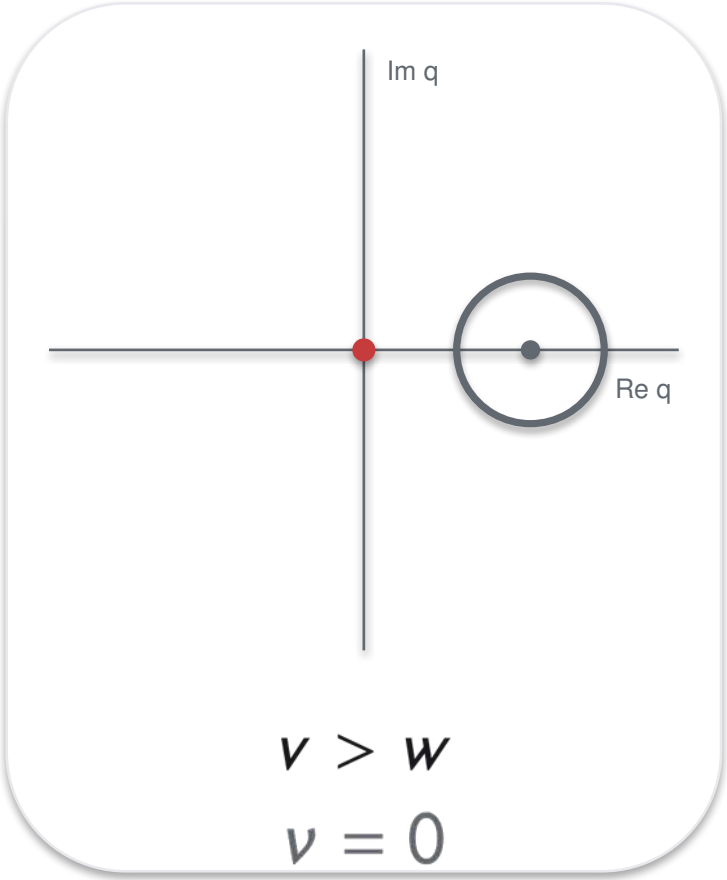

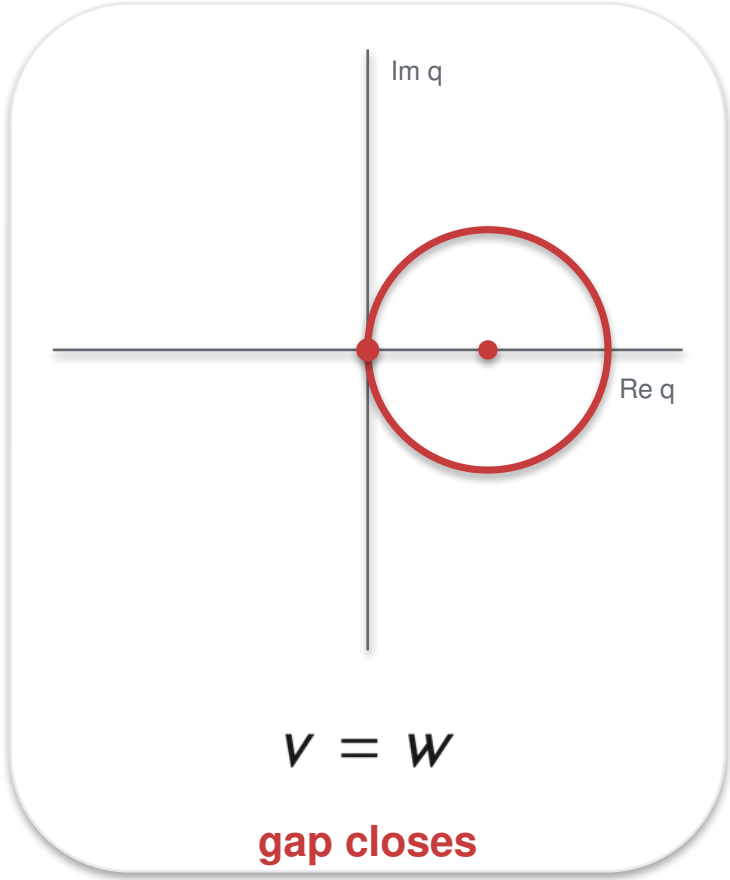

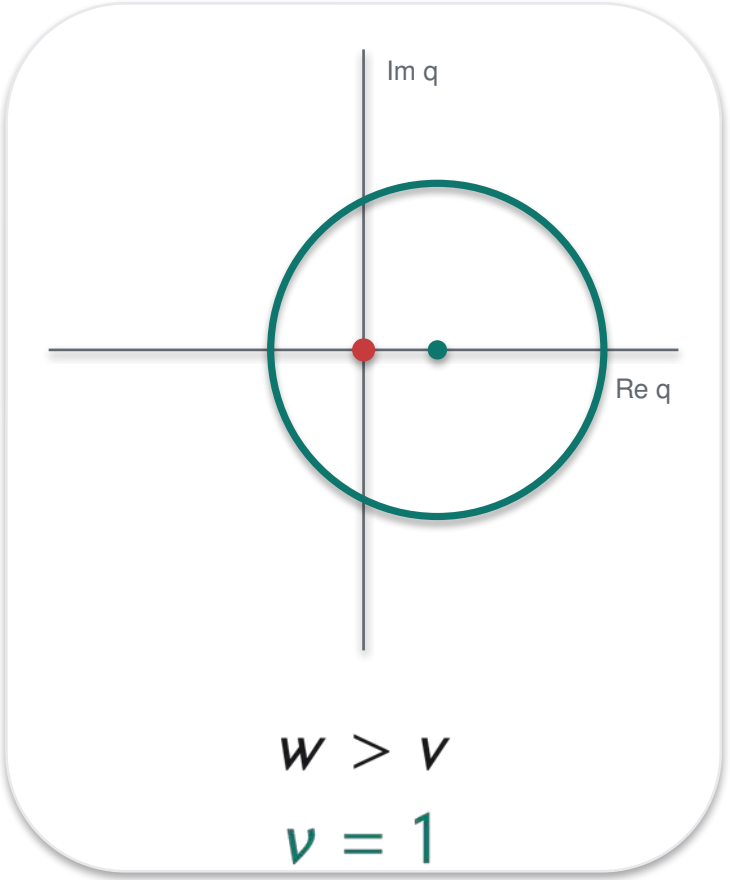

Checkpoint: diagnose the phase without diagonalizing H

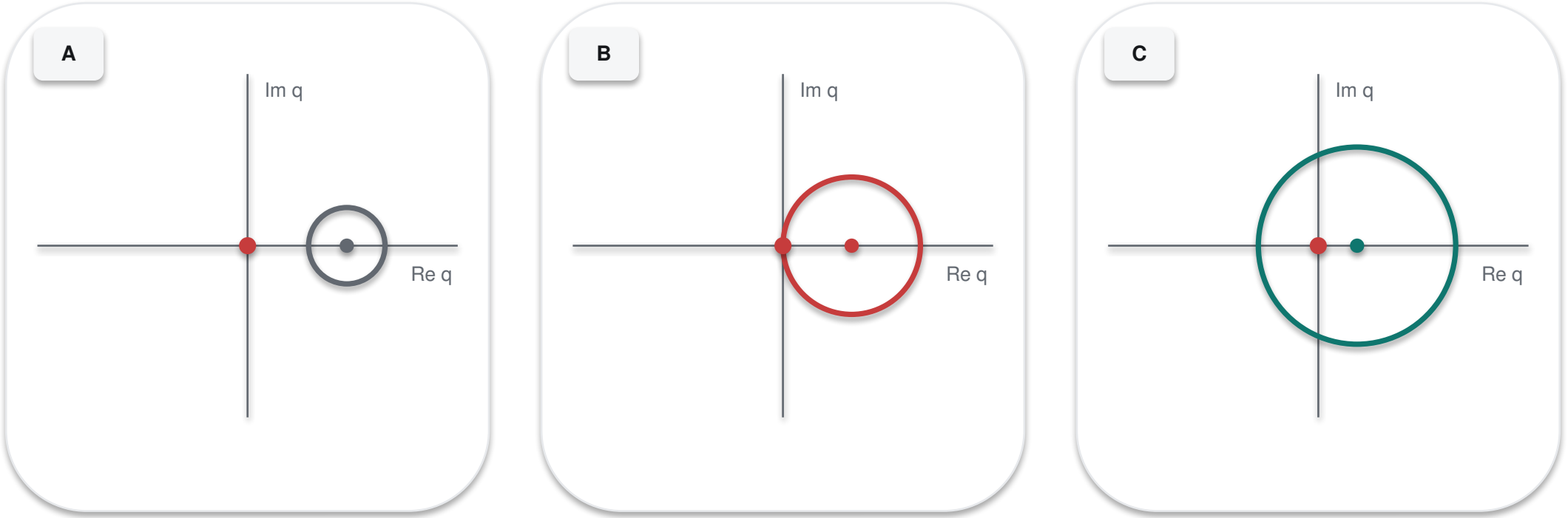

For each path: Is the system gapped? What is the winding number?

What must happen before A can become C?

Topology ignores shape, but not the gap

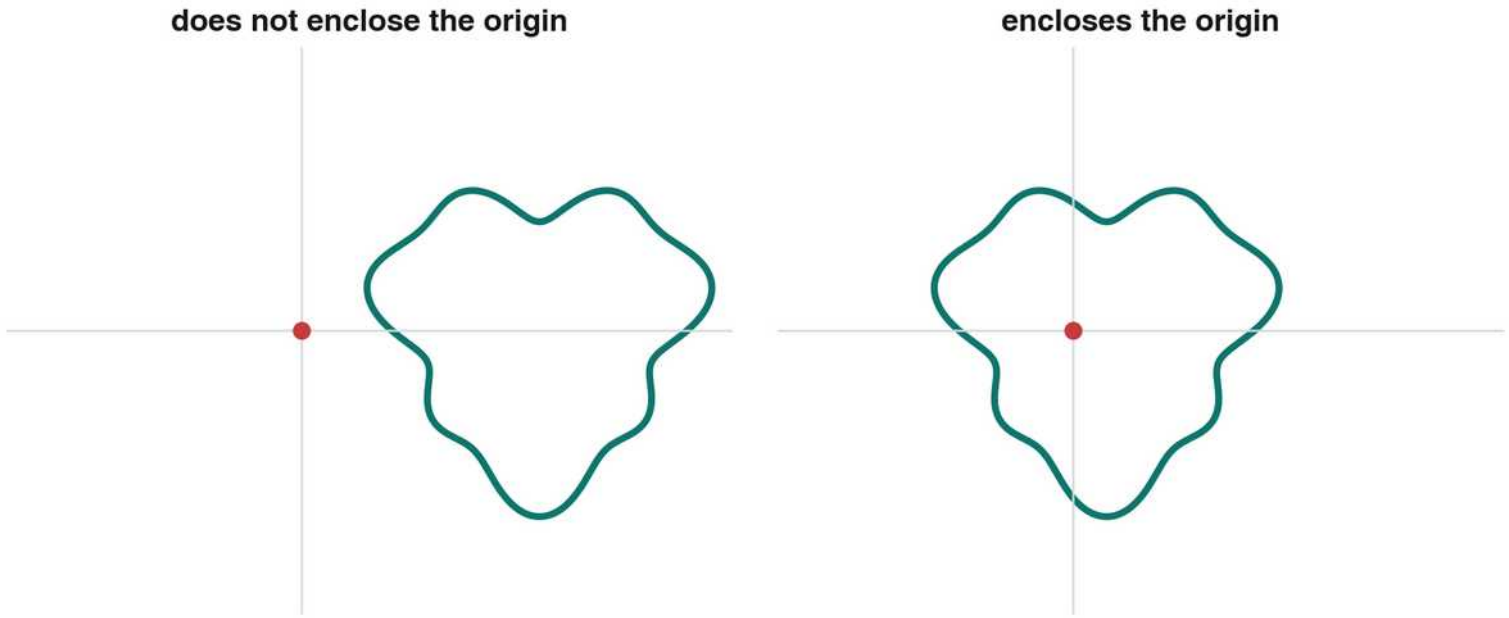

Allowed deformations

- change v and w smoothly
- distort the loop
- add longer-range A–B bonds

Forbidden shortcut

cross the origin while remaining an insulator

Different winding numbers label disconnected sets of gapped Hamiltonians.

The phase diagram: two islands that cannot touch

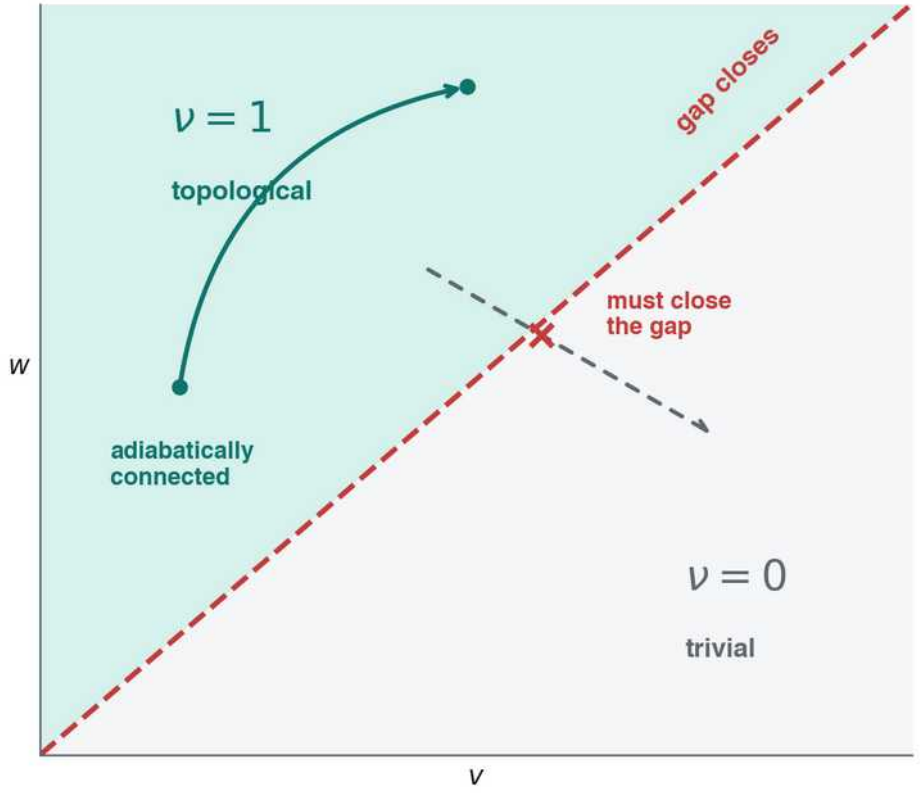

What makes ν a topological invariant?

- it is an integer computed from the gapped bulk
- it cannot change under deformations that keep the gap open and respect chiral symmetry
- so it can only change where the gap closes: the line v = w

Any two chains inside the same region are adiabatically connected: they are one phase.

The bulk invariant meets a physical boundary

Periodic boundary conditions

Bloch bands and winding

Open boundary conditions

possible boundary-localized states

Bulk–boundary correspondence asks whether the bulk winding predicts the boundary spectrum.

The open chain develops in-gap states

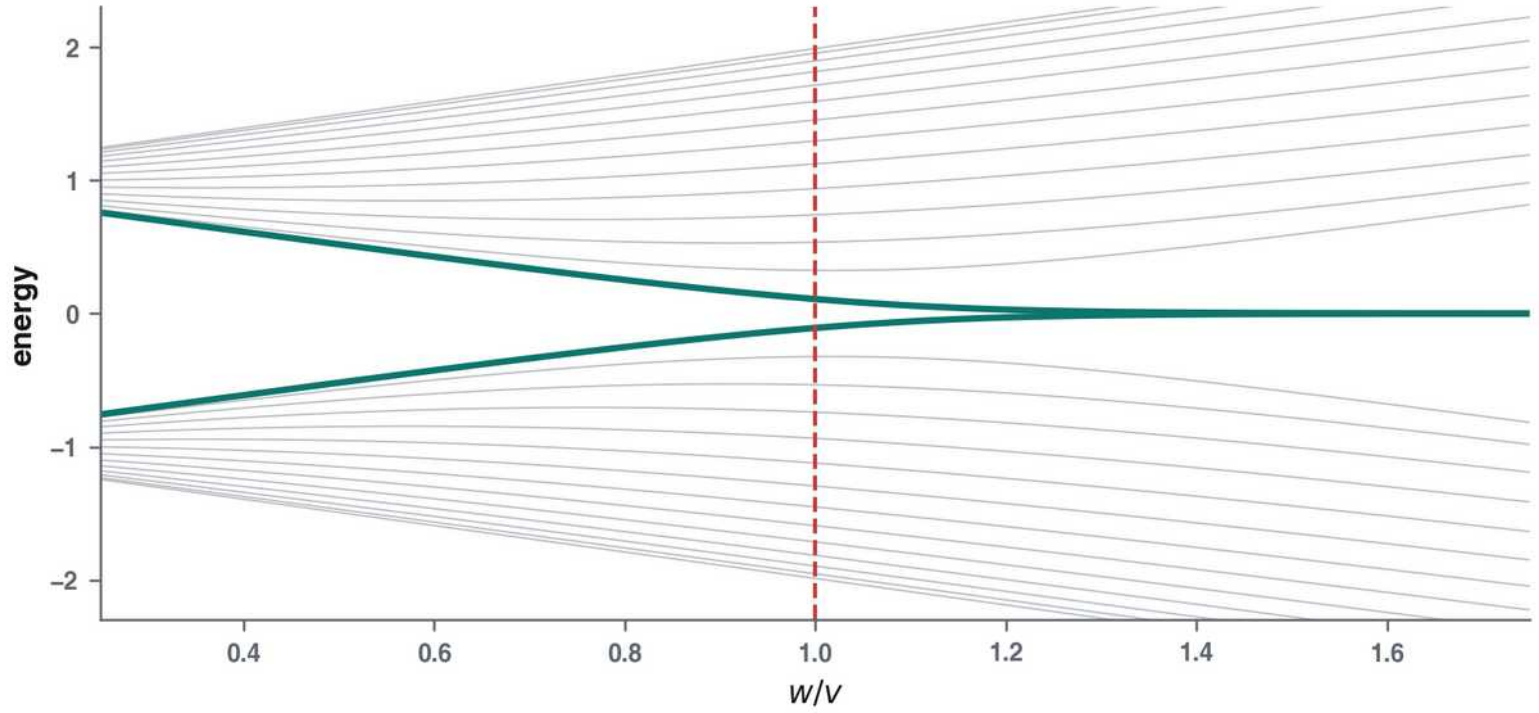

In the nontrivial regime

- the bulk remains gapped
- two states approach zero energy
- here N = 14 cells — the pair hugs zero as w/v grows

The new states have no periodic-bulk counterpart.

The in-gap states live at the ends

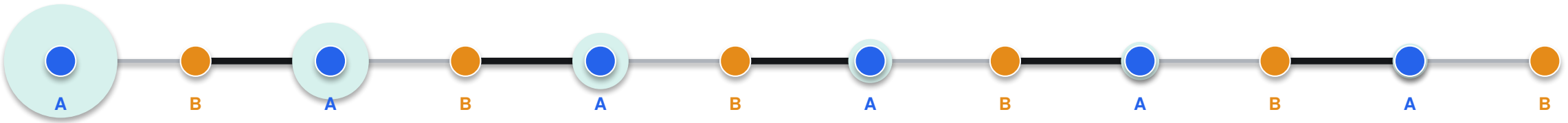

left-edge mode: amplitude only on the A sublattice

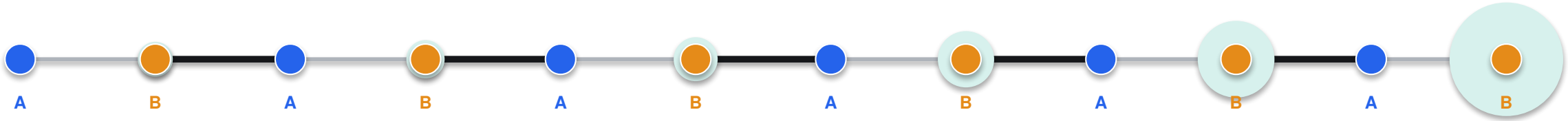

right-edge mode: amplitude only on the B sublattice

Localization and sublattice polarization follow directly from zero energy and chiral symmetry.

Deriving the left-edge state

open end

At zero energy, choose

$$b_n = 0$$

$$v\,a_n + w\,a_{n+1} = 0 \quad \Longrightarrow \quad a_{n+1} = -\frac{v}{w}\,a_n$$

Each unit cell multiplies the amplitude by the negative hopping ratio.

Normalizability selects the topological regime

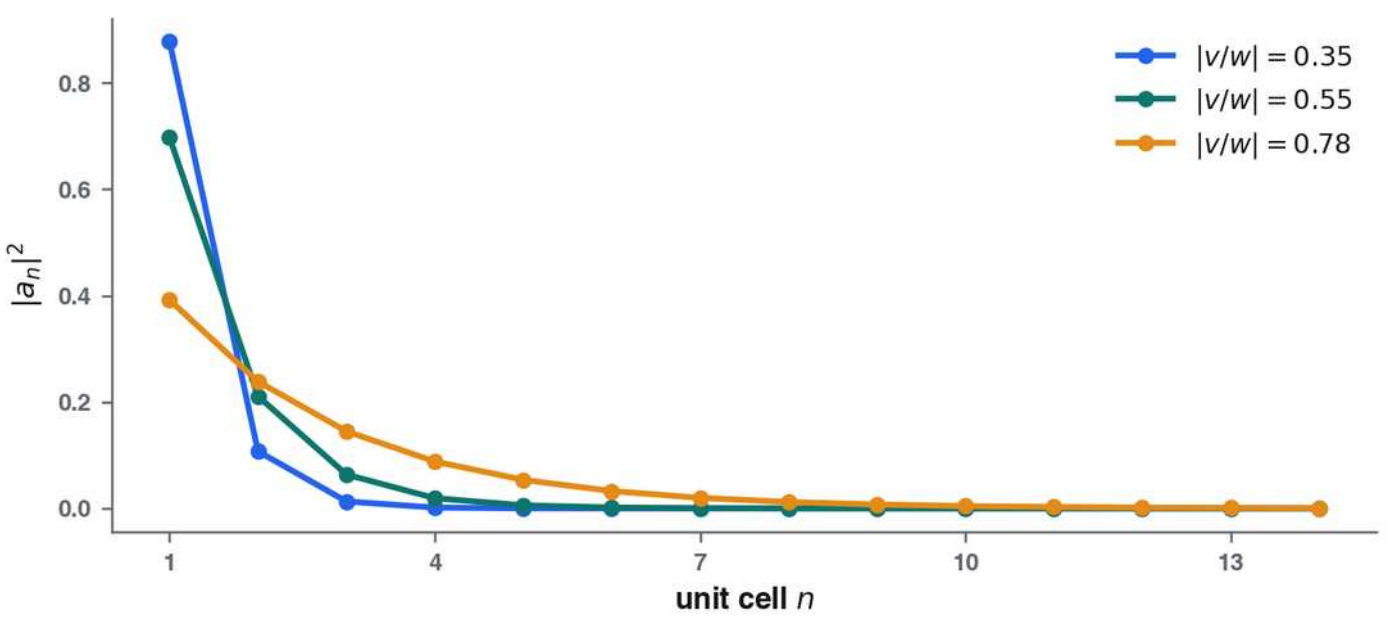

$$a_n \propto \left(-\frac{v}{w}\right)^{n-1}$$

$$\left|\frac{v}{w}\right| < 1$$

normalizable $\iff$ $w > v$

$$\xi^{-1} = \ln\left|\frac{w}{v}\right|$$

The edge-state condition is exactly the nontrivial bulk winding condition.

Finite chains: the two ends can talk to each other

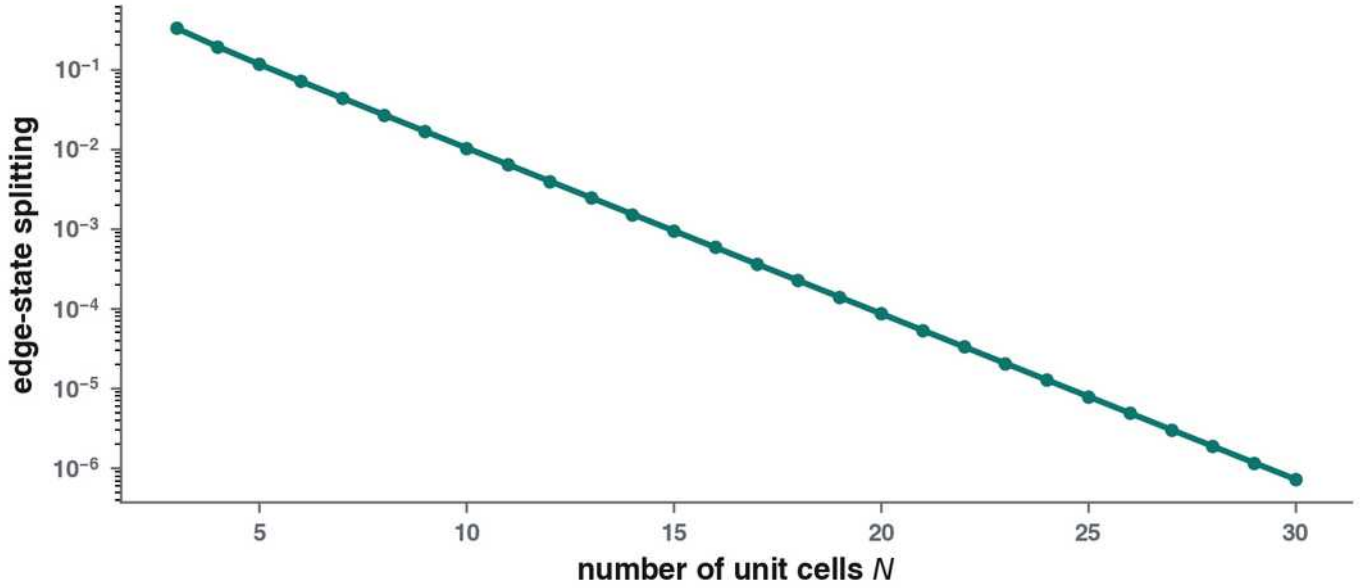

$$\Delta E \sim e^{-L/\xi}$$

- two near-zero levels at opposite energies
- the splitting vanishes exponentially with length

Exact zero energy is recovered in the semi-infinite limit.

An interface makes bulk–boundary correspondence explicit

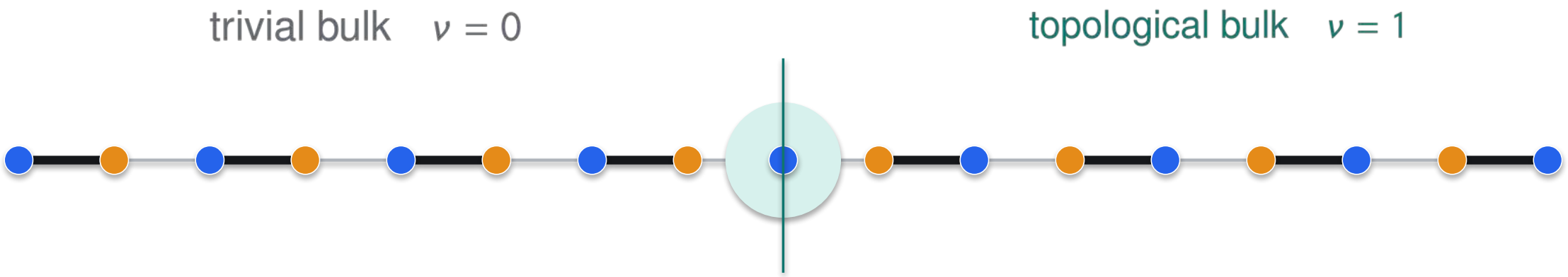

$$N_{\text{interface}} = \left|\nu_{\text{right}} - \nu_{\text{left}}\right|$$

In polyacetylene, this is the soliton associated with a change of dimerization.

The boundary state does not require a perfect lattice

random hopping — still only between A and B

What is preserved?

- chiral symmetry
- a bulk or mobility gap
- the interface winding mismatch

What can remove the state?

- closing the relevant bulk gap
- breaking the protecting symmetry
- annihilating it with another mode

Without chiral symmetry, the loop can escape

Add a staggered onsite potential

$$H(k) \longrightarrow H(k) + m\sigma_z$$

- the chiral anticommutator no longer vanishes
- a nonzero out-of-plane component is now allowed
- the path can leave the plane

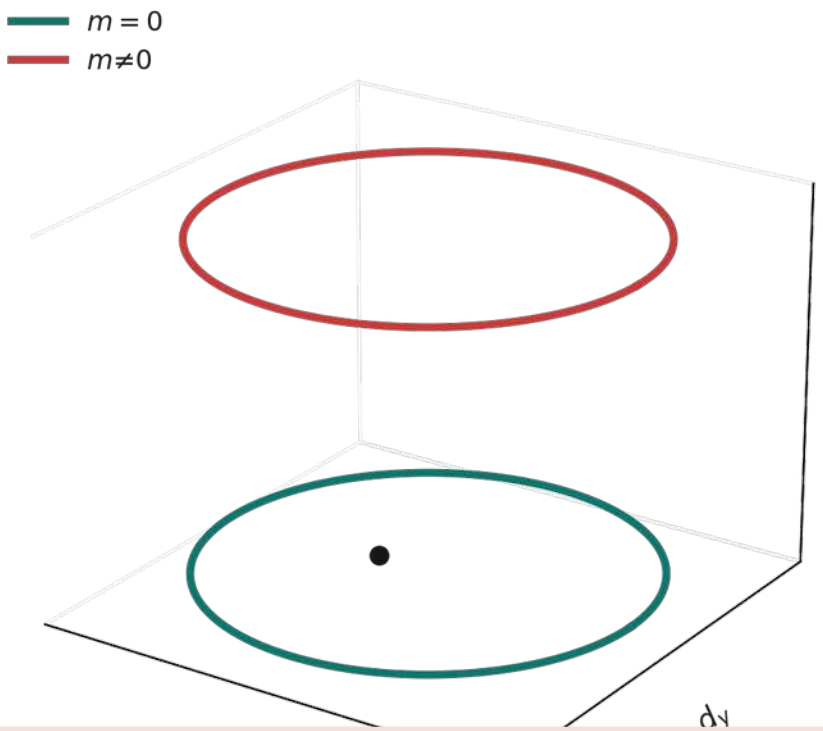

Once the planar constraint is removed, the loop can be contracted without reaching the origin.

A subtle point: unit cell and termination move together

Choice 1: group A and B in the same cell

Choice 2: shift the cell boundary by one site

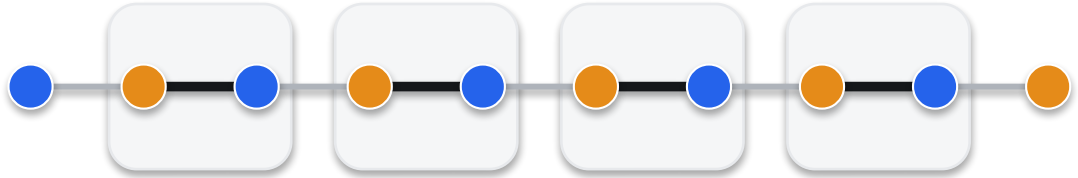

A relabeling may shift the numerical winding — but it also shifts where the chain is cut.

- compare two bulks using one consistent convention
- the invariant content is the difference across a physical interface
- polarization is defined modulo one electron charge

No unit-cell convention creates a physical edge state by itself.

The SSH diagnostic card

BULK HAMILTONIAN	$H(k) = d_x\sigma_x + d_y\sigma_y$
PROTECTING CONSTRAINT	chiral symmetry $\quad \{\Gamma, H\} = 0$
BULK INVARIANT	winding number $\quad \nu \in \mathbb{Z}$
PHASE TRANSITION	the bulk gap closes when the hoppings become equal
BOUNDARY PREDICTION	zero-energy end or interface mode
PHYSICAL LANGUAGE	polarization · end charge · soliton

Topology is an obstruction to connecting gapped Hamiltonians while respecting the symmetry.

Further reading: J. K. Asbóth, L. Oroszlány & A. Pályi, A Short Course on Topological Insulators, Lect. Notes Phys. 919 (Springer, 2016) · arXiv:1509.02295

NEXT LECTURE

From a one-dimensional winding to a two-dimensional response

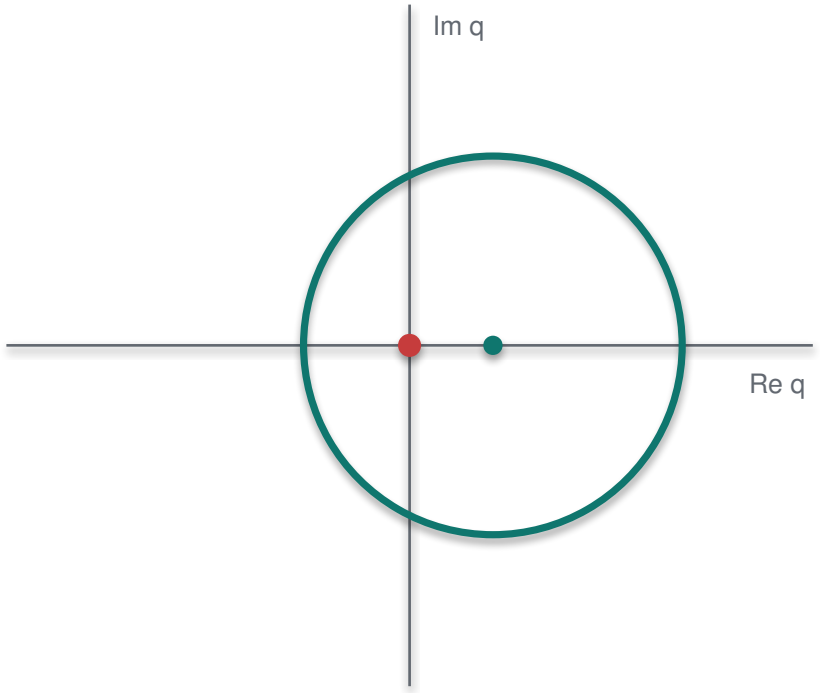

1D BZ → winding

2D bulk → conducting edge?

Why can the winding not change continuously? · What replaces it in two dimensions?

Next: A primer on graphene's bandstructure
the integer Quantum Hall effect

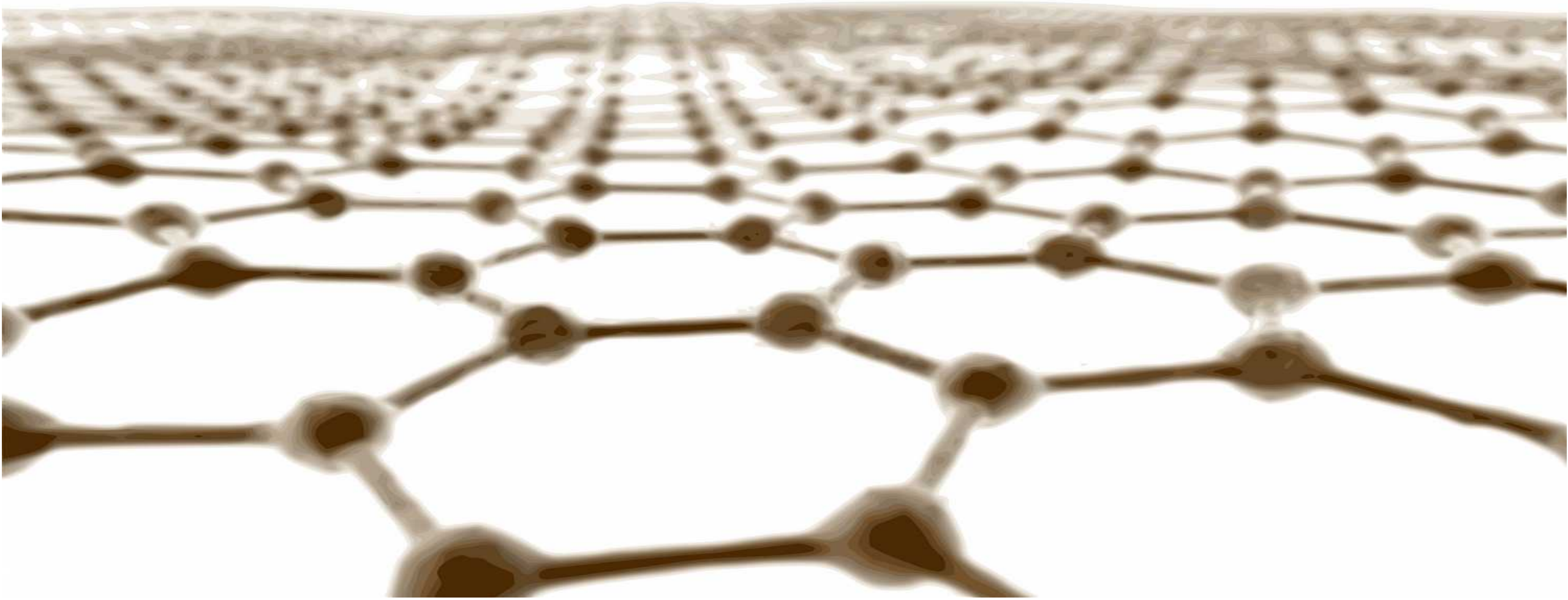

Graphene’s bandstructure

Luis E. F. Foà Torres

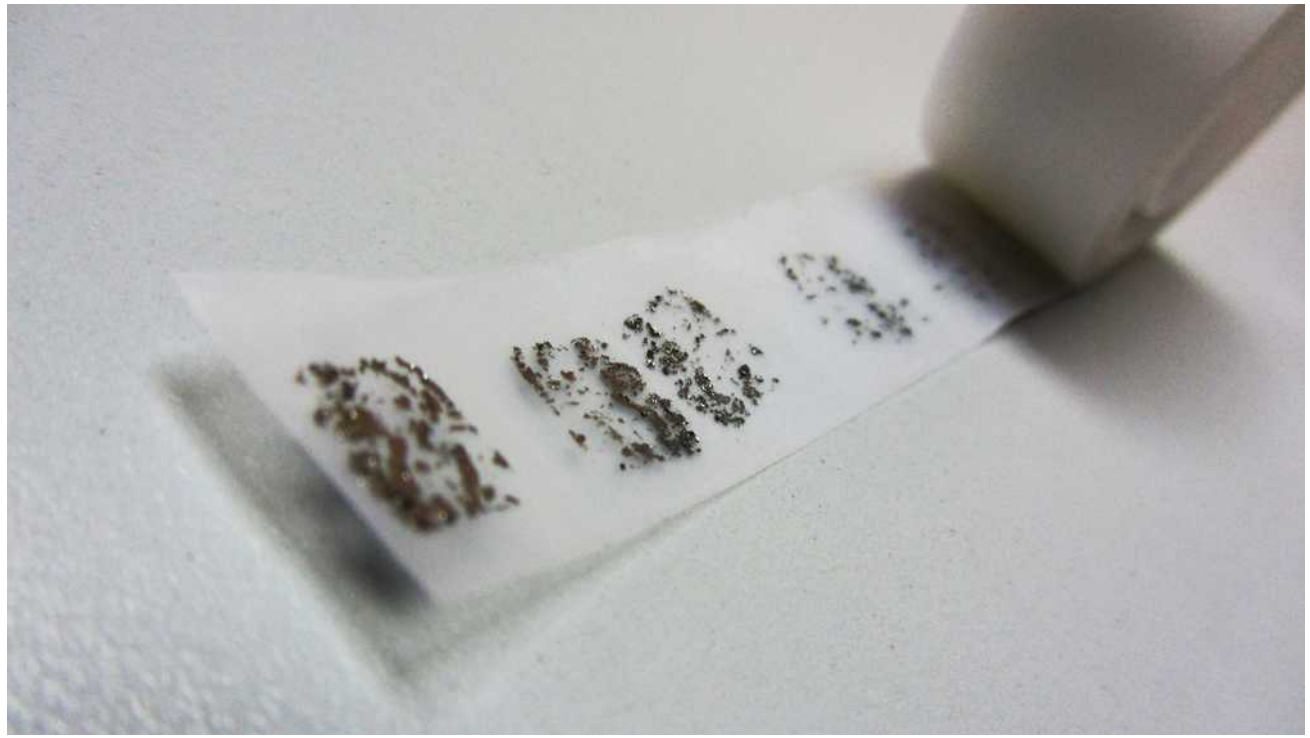

All the material from these lectures will be here:

Graphene's peculiar electronic structure

Pi orbitals matter most

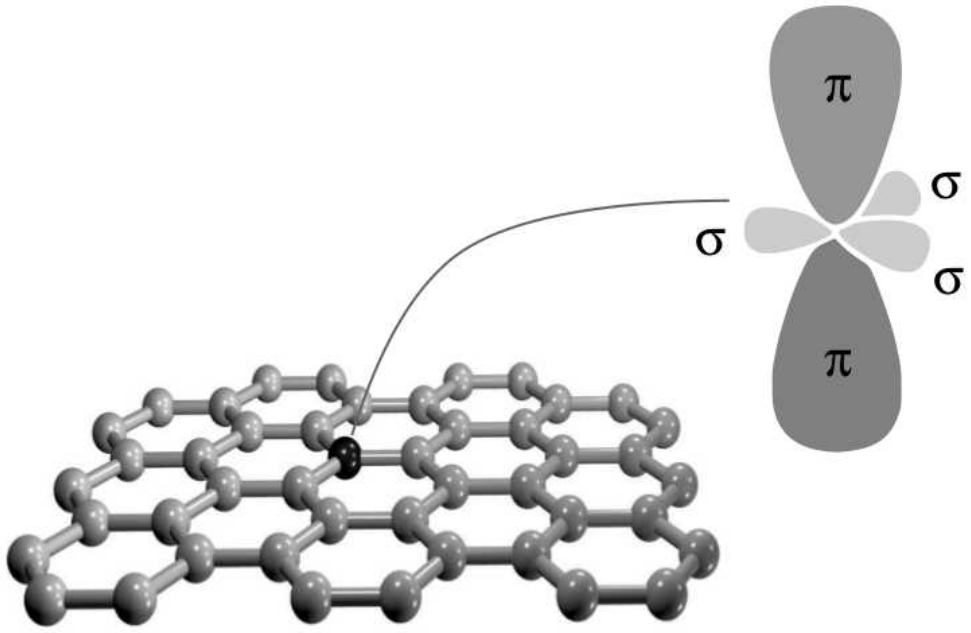

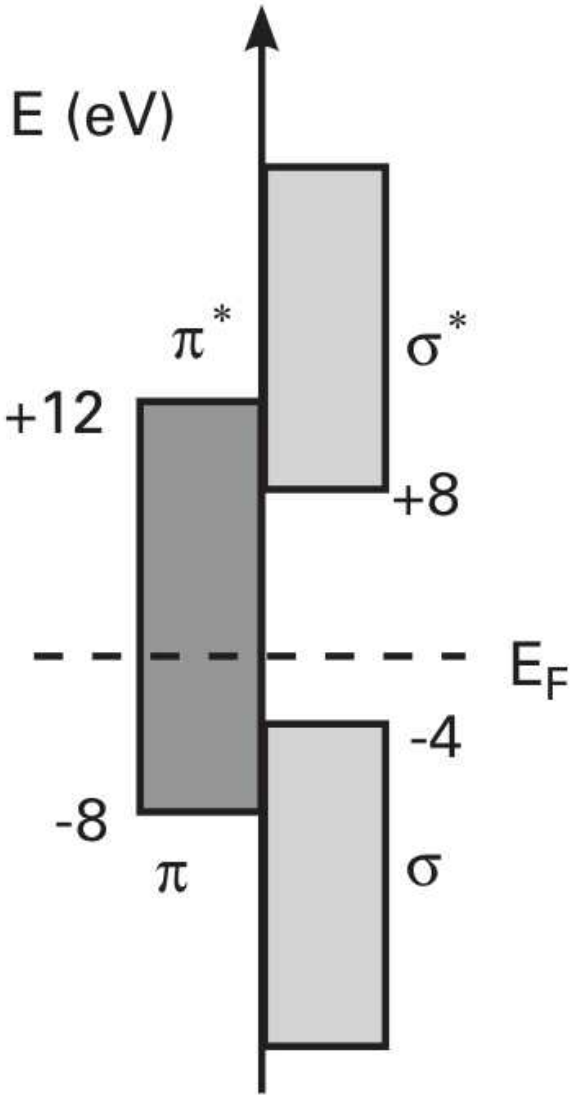

Foa Torres, S. Roche, J-C Charlier, *"Introduction to Graphene-based nanomaterials"*, Cambridge University Press (2014).

Real space lattice

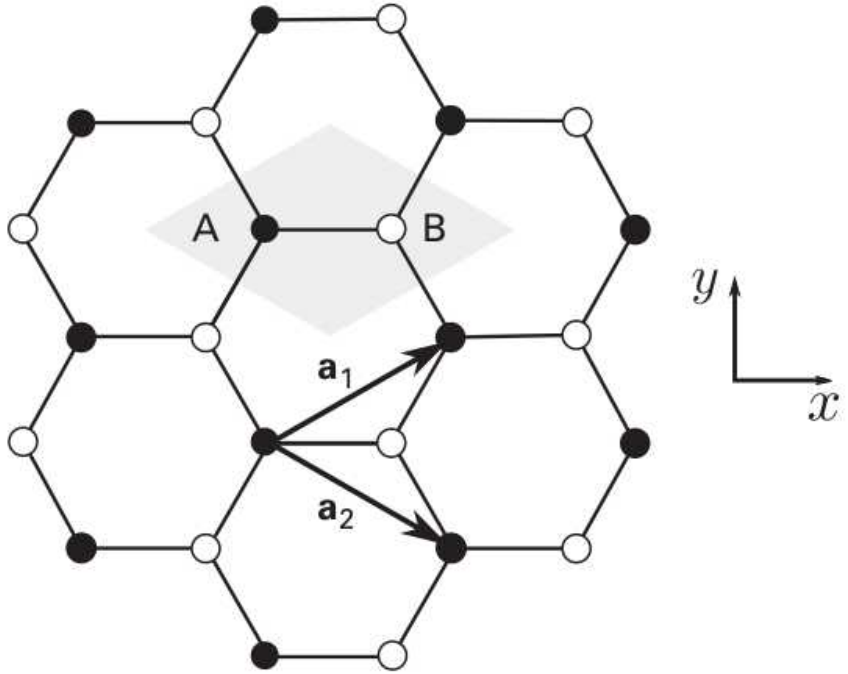

Reciprocal space

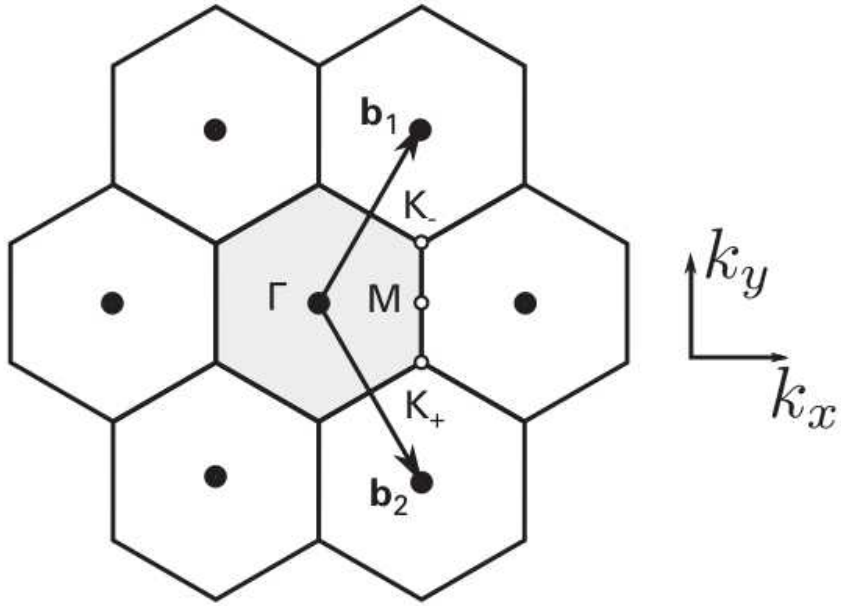

Triangular Bravais lattice with a basis

Real space lattice

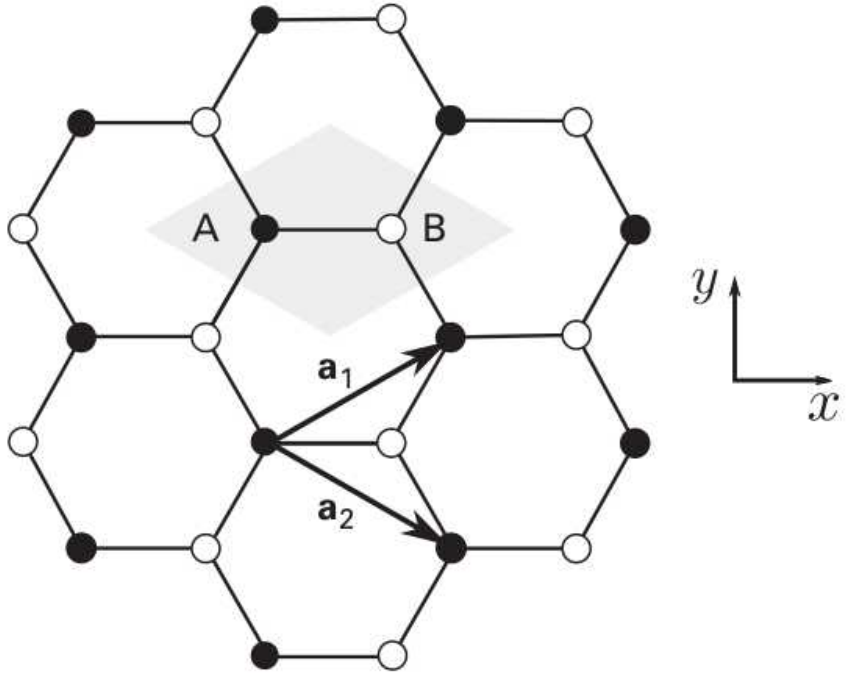

Reciprocal space

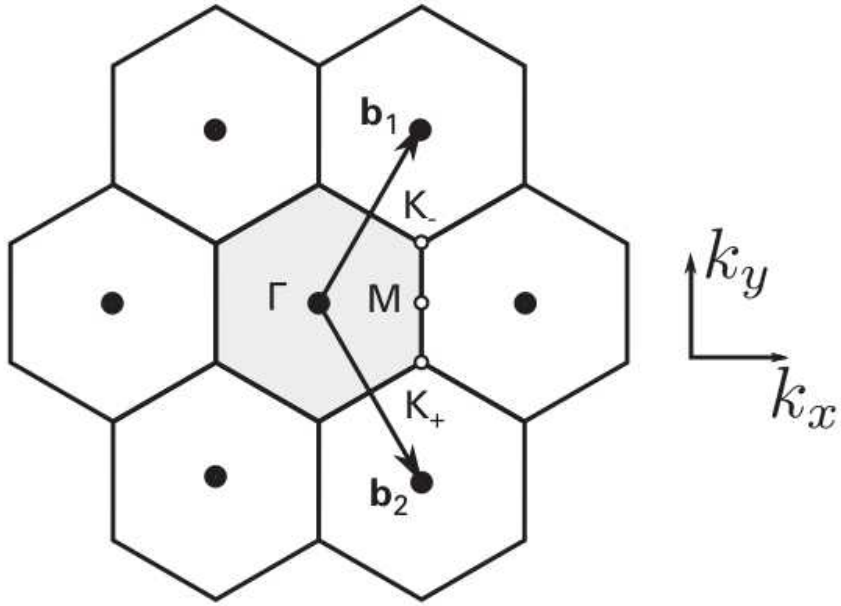

Triangular Bravais lattice with a basis

Bloch's Theorem + tight-binding approx.

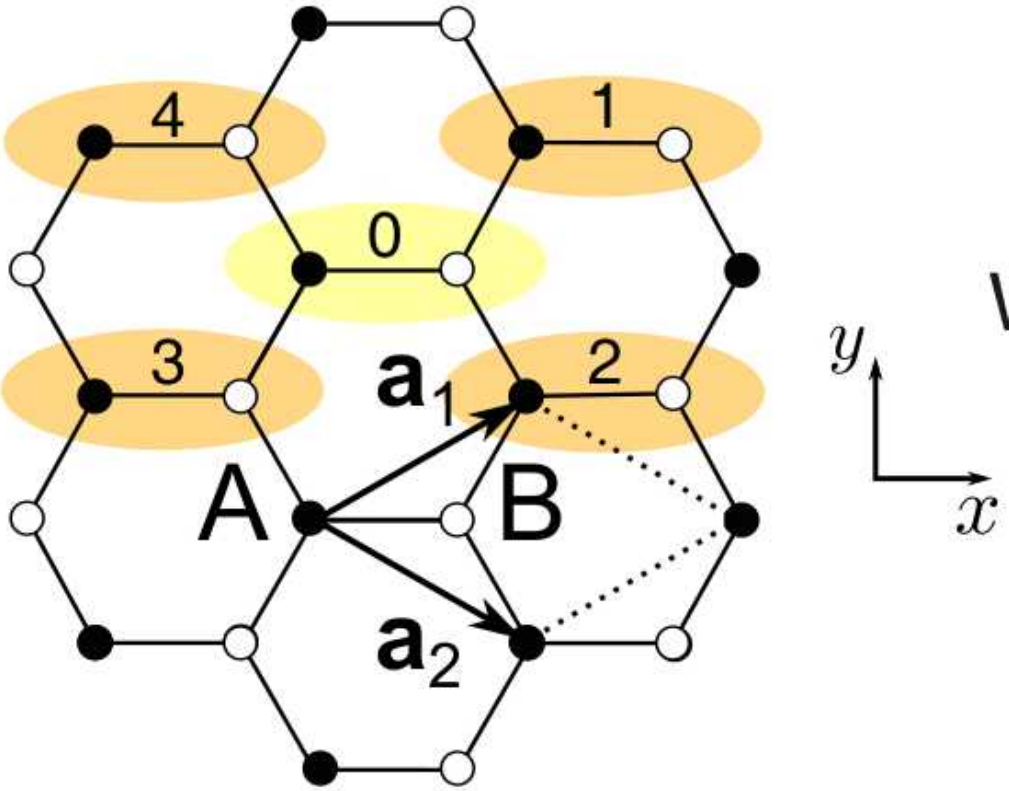

1

We draw the graphene lattice highlighting a central cell and its neighbors.

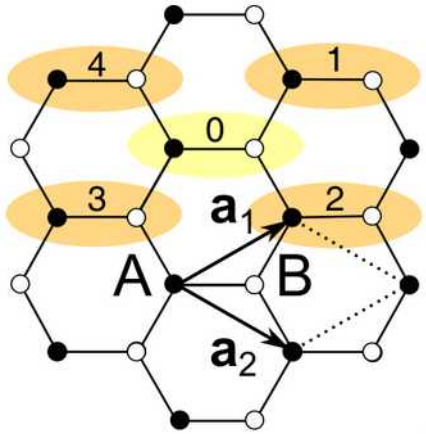

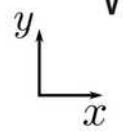

1

We draw the graphene lattice highlighting a central cell and its neighbors.

we got two indexes:
cell index atom type

3A 3B 4A 4B 0A 0B 1A 1B 2A 2B

2

Now we write the Hamiltonian in matrix form.
Since we have a single orbital per atom
we got a one to one correspondence between
orbitals and their space position.

Assembling
the Hamiltonian
is very much like
playing Battleship
(or *"Batalla Naval"*
as is known in Spain).

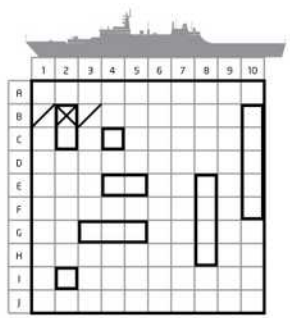

3A
3B
4A
4B
0A
0B
1A
1B
2A
2B

$$\begin{array}{cc} 0 & -\gamma_0 \\ -\gamma_0 & 0 \end{array}$$

For example, this is the matrix element connecting sites 3B with 0A

3 Now we write the time-independent Schrödinger equation using Bloch's theorem for the wave-functions.

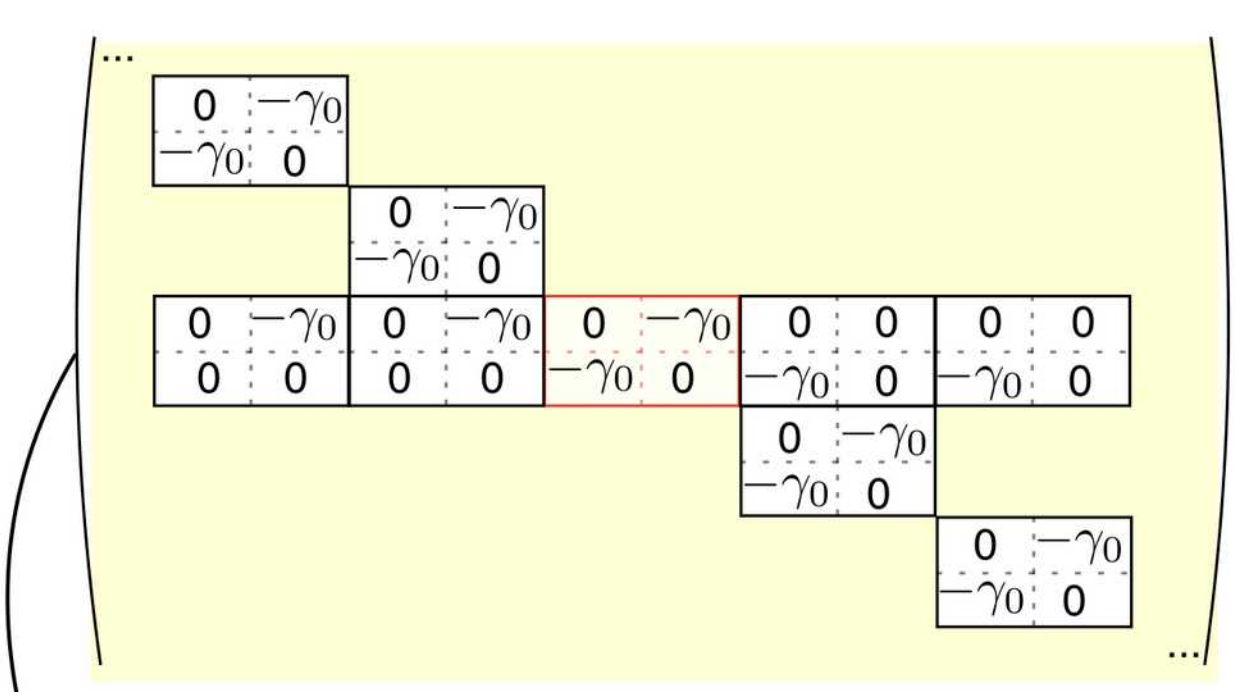

$$
\begin{pmatrix}
\vdots \\
c_A e^{ik\cdot(R_3-R_0)} \\
c_B e^{ik\cdot(R_3-R_0)} \\
c_A e^{ik\cdot(R_4-R_0)} \\
c_B e^{ik\cdot(R_4-R_0)} \\
c_A \\
c_B \\
c_A e^{ik\cdot(R_1-R_0)} \\
c_B e^{ik\cdot(R_1-R_0)} \\
c_A e^{ik\cdot(R_2-R_0)} \\
c_B e^{ik\cdot(R_2-R_0)} \\
\vdots
\end{pmatrix}
= \varepsilon_k
\begin{pmatrix}
\vdots \\
c_A e^{ik\cdot(R_3-R_0)} \\
c_B e^{ik\cdot(R_3-R_0)} \\
c_A e^{ik\cdot(R_4-R_0)} \\
c_B e^{ik\cdot(R_4-R_0)} \\
c_A \\
c_B \\
c_A e^{ik\cdot(R_1-R_0)} \\
c_B e^{ik\cdot(R_1-R_0)} \\
c_A e^{ik\cdot(R_2-R_0)} \\
c_B e^{ik\cdot(R_2-R_0)} \\
\vdots
\end{pmatrix}
$$

3 Now we write the time-independent Schrödinger equation using Bloch's theorem for the wave-functions.

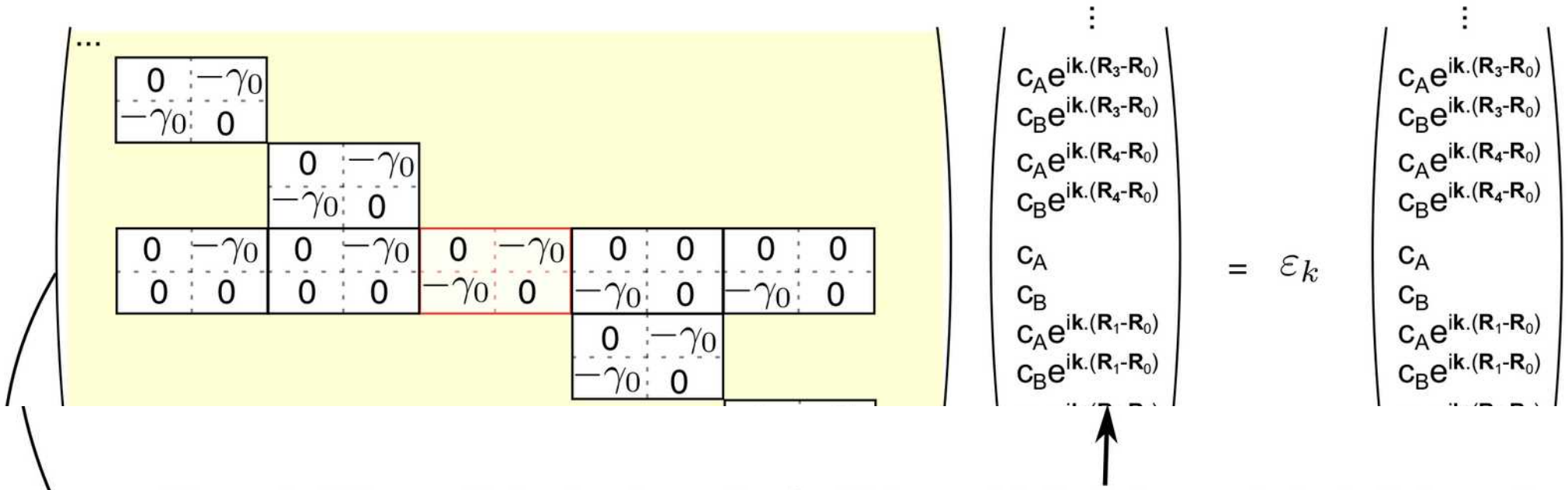

The probability amplitude at a given site of cell j is equal to that at an equivalent site in another cell but multiplied by a phase.

4

$$\begin{cases} -\gamma_0\ c_B e^{ik.(R_4-R_0)} - \gamma_0\ c_B e^{ik.(R_3-R_0)} - \gamma_0\ c_B = \varepsilon_k\ c_A \\ -\gamma_0\ c_A - \gamma_0\ c_A e^{ik.(R_1-R_0)} - \gamma_0\ c_A e^{ik.(R_2-R_0)} = \varepsilon_k\ c_B \end{cases}$$

$R_4-R_0=-a_2$
$R_1-R_0= a_1$
...

After some algebra one gets Eq. (2.16) for the dispersion:

$$E_{\pm}(k_x,k_y) = \pm\gamma_0\sqrt{1+4\cos\frac{\sqrt{3}k_x a}{2}\cos\frac{k_y a}{2}+4\cos^2\frac{k_y a}{2}}.$$

Bandstructure and low-energy approximation

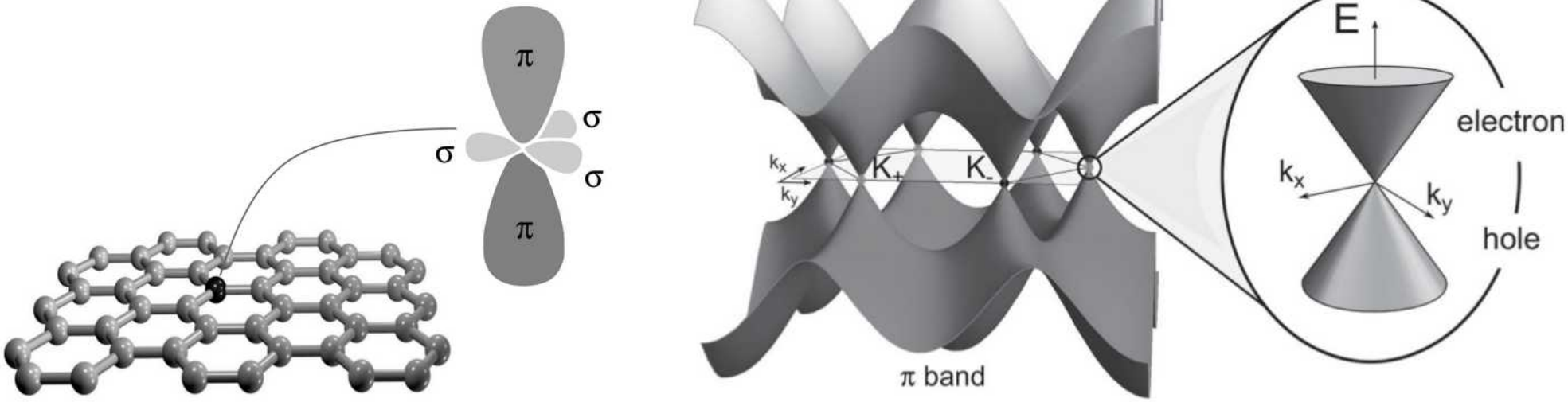

Technically, a zero-bandgap semiconductor.

Bandstructure and low-energy approximation

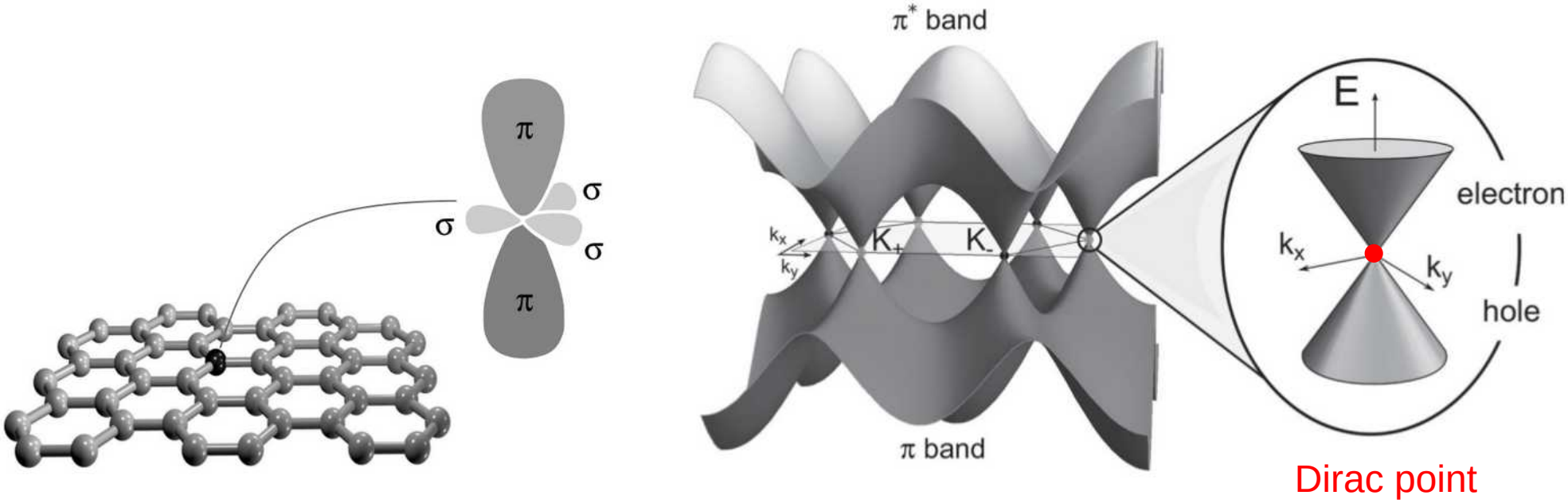

Dirac point is not accidental,
it's protected by symmetries.
Time-reversal (broken by a magnetic field)
and inversion symmetry (broken by a potential which distinguishes A from B-type atoms).

See Exercises 2.2 and 2.16

Bandstructure and low-energy approximation

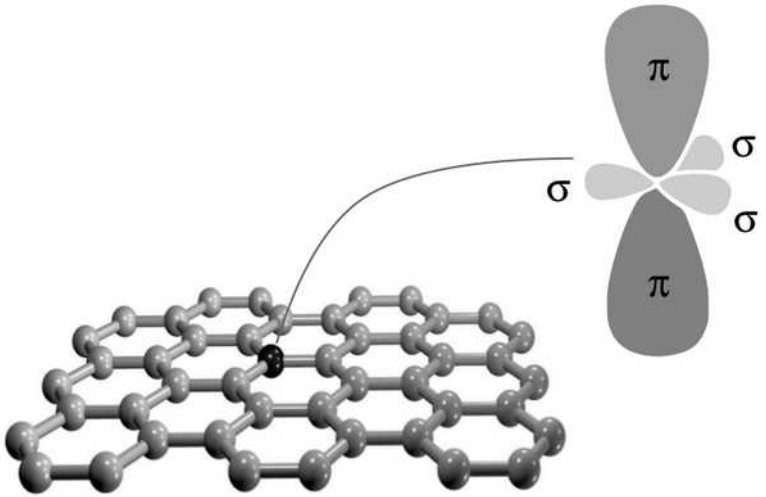

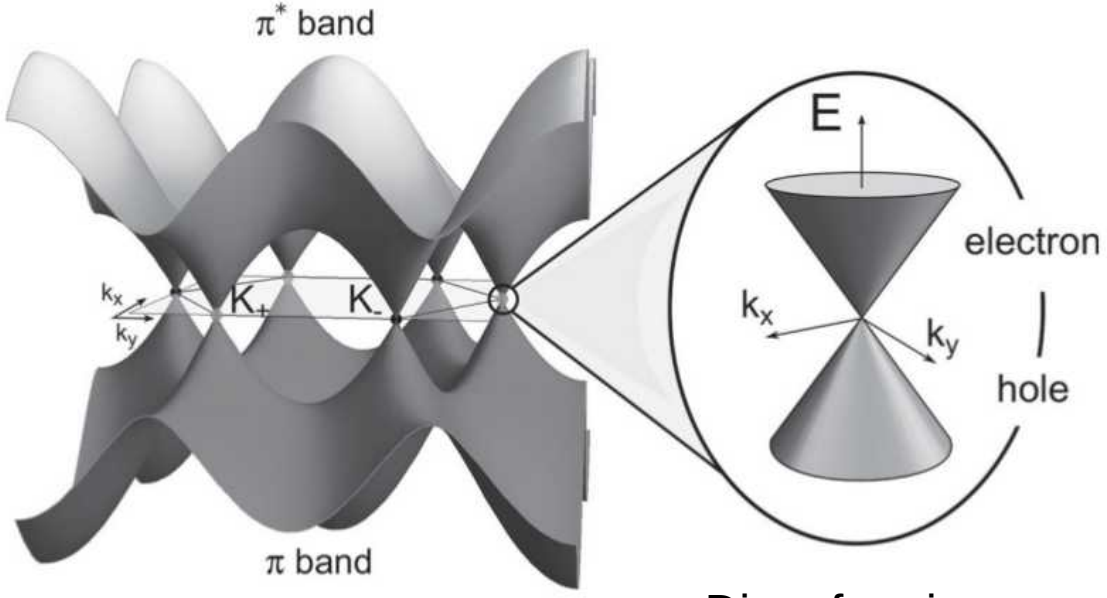

Dirac fermions

$$\mathcal{H}_{K_+} = \hbar v_F \begin{pmatrix} 0 & k_x - ik_y \\ k_x + ik_y & 0 \end{pmatrix}$$

Bandstructure and low-energy approximation

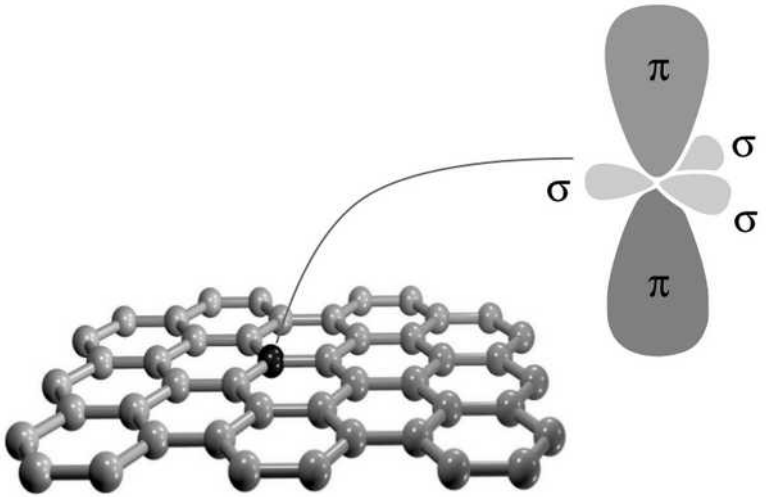

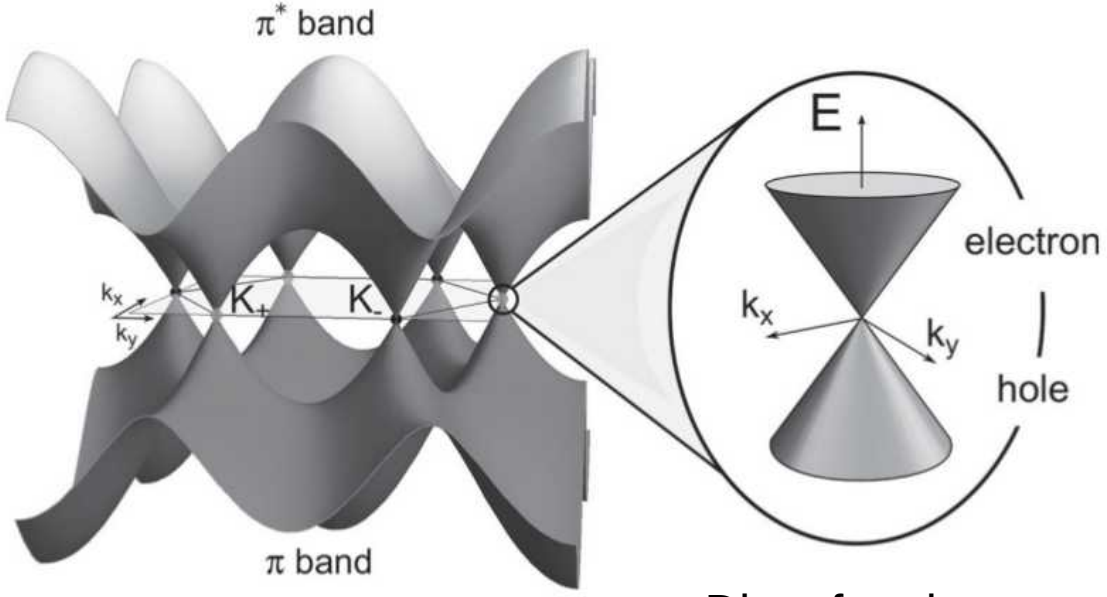

Dirac fermions

$$\mathcal{H}_{K_+} = \hbar v_F \begin{pmatrix} 0 & k_x - ik_y \\ k_x + ik_y & 0 \end{pmatrix} = v_F(p_x\sigma_x + p_y\sigma_y),$$

Pauli matrices

$$\sigma_x = \begin{pmatrix} 0 & 1 \\ 1 & 0 \end{pmatrix}, \quad \sigma_y = \begin{pmatrix} 0 & -i \\ i & 0 \end{pmatrix}, \quad \sigma_z = \begin{pmatrix} 1 & 0 \\ 0 & -1 \end{pmatrix}$$

Bandstructure and low-energy approximation

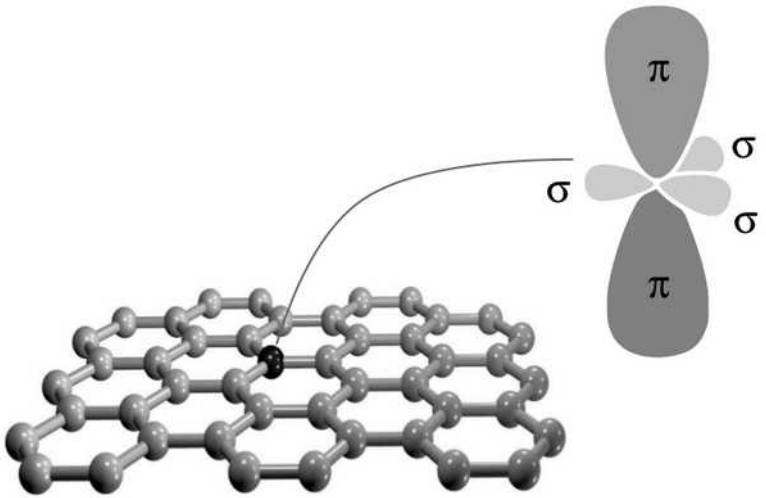

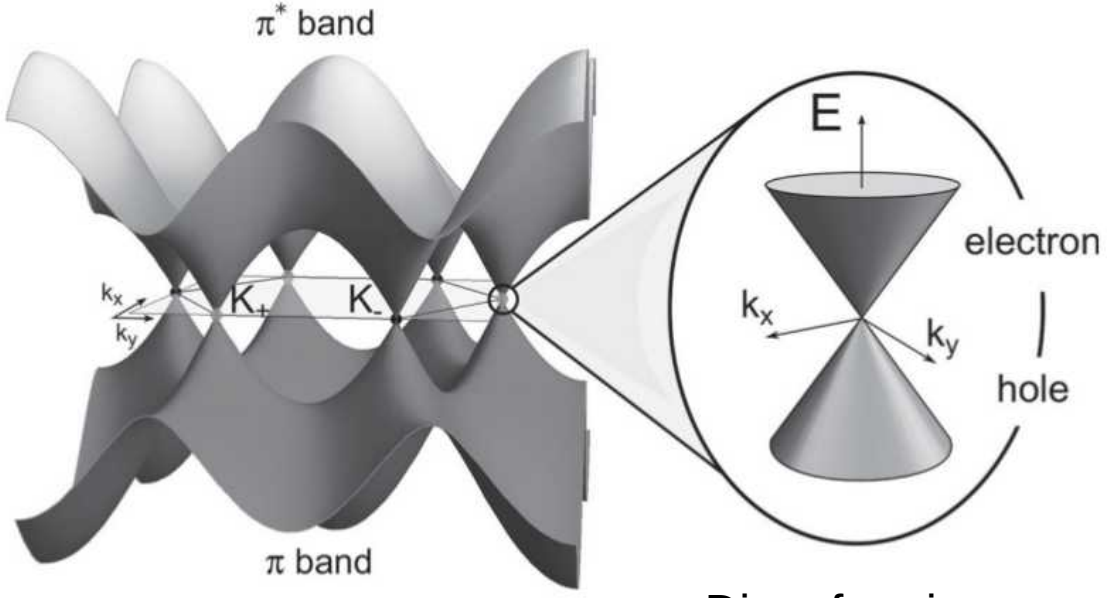

Dirac fermions

$$\mathcal{H}_{K_+} = \hbar v_F \begin{pmatrix} 0 & k_x - ik_y \\ k_x + ik_y & 0 \end{pmatrix}$$

$$= v_F(p_x\sigma_x + p_y\sigma_y),$$

$$\hat{\sigma} = (\sigma_x, \sigma_y, \sigma_z) \qquad \mathcal{H}_{K_+} = v_F\hat{\sigma}.\mathbf{p},$$

Bandstructure and low-energy approximation

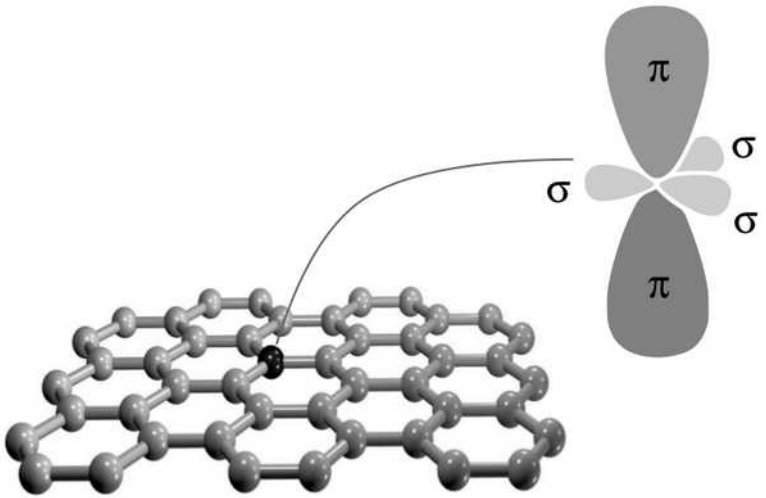

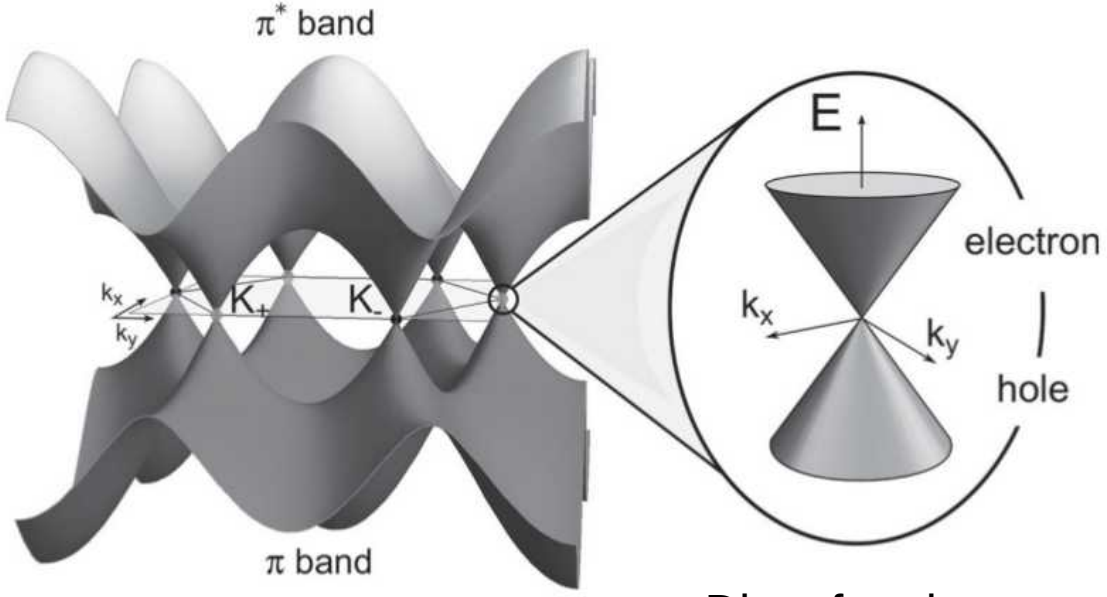

Dirac fermions

The state-vector has a spinor structure

$$\mathcal{H}_{K_+} = \hbar v_F \begin{pmatrix} 0 & k_x - ik_y \\ k_x + ik_y & 0 \end{pmatrix}$$

$$= v_F(p_x\sigma_x + p_y\sigma_y),$$

$$\hat{\sigma} = (\sigma_x, \sigma_y, \sigma_z)$$

$$\mathcal{H}_{K_+} = v_F \hat{\sigma}.\mathbf{p},$$

Bandstructure and low-energy approximation

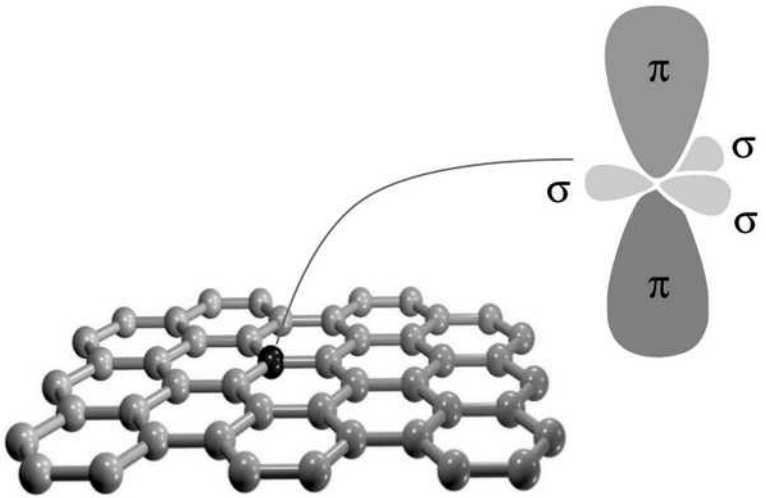

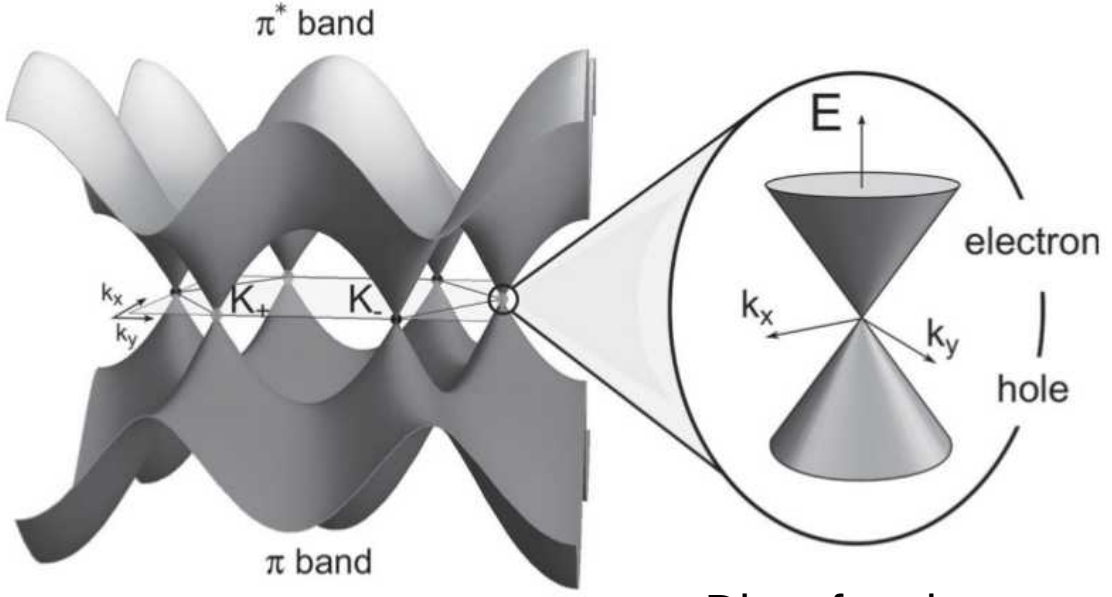

Dirac fermions

Relativistic-like particles with ZERO REST MASS but “low” speed

$v_F = 10^6$ m/s ±5%

$$\hat{\sigma} = (\sigma_x, \sigma_y, \sigma_z)$$

$$\mathcal{H}_{K_+} = \hbar v_F \begin{pmatrix} 0 & k_x - ik_y \\ k_x + ik_y & 0 \end{pmatrix}$$

$$= v_F(p_x\sigma_x + p_y\sigma_y),$$

$$\mathcal{H}_{K_+} = v_F \hat{\sigma} . \mathbf{p},$$

Bandstructure and low-energy approximation

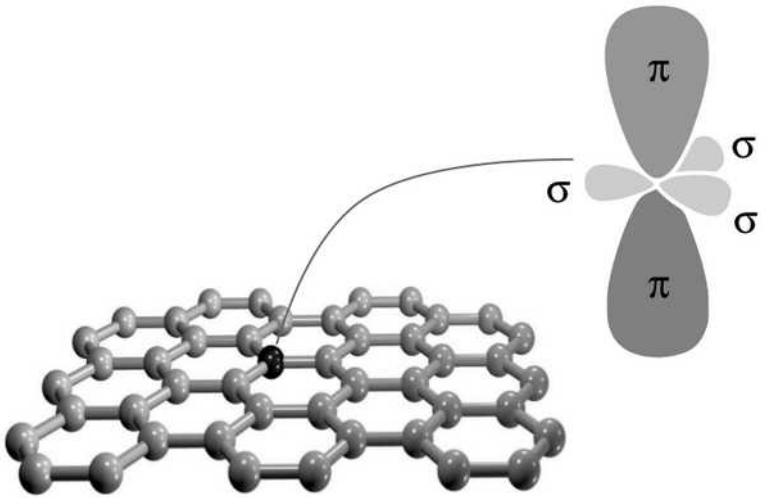

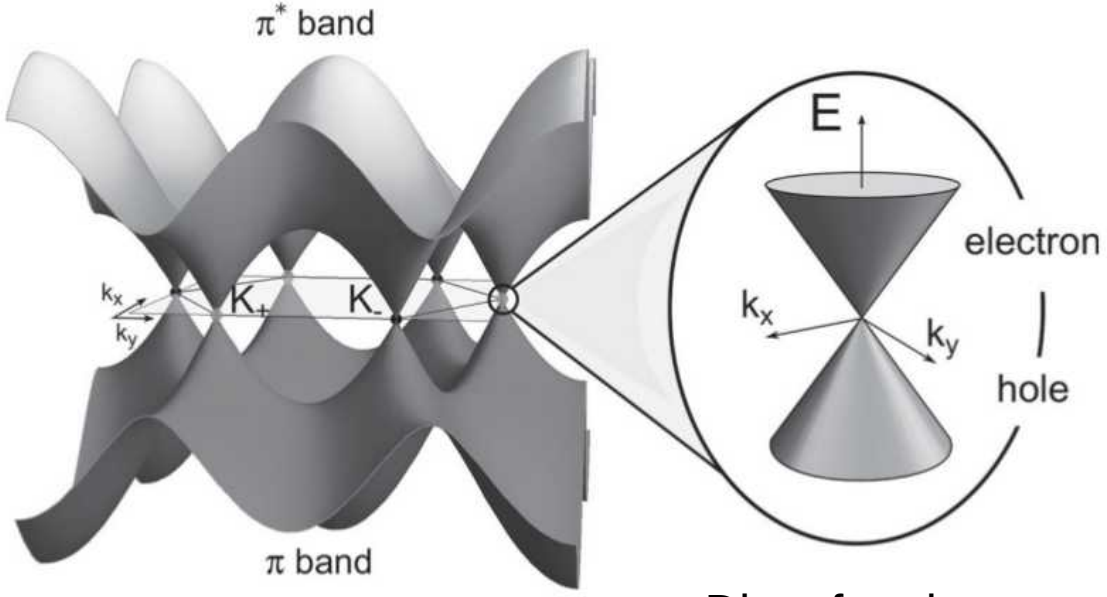

Dirac fermions

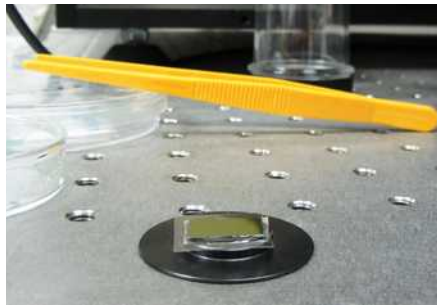

"CERN on a Desk"
A. Geim

$$\hat{\sigma} = (\sigma_x, \sigma_y, \sigma_z)$$

$$\mathcal{H}_{K_+} = \hbar v_F \begin{pmatrix} 0 & k_x - ik_y \\ k_x + ik_y & 0 \end{pmatrix}$$

$$= v_F(p_x\sigma_x + p_y\sigma_y),$$

$$\mathcal{H}_{K_+} = v_F \hat{\sigma} . \mathbf{p},$$

Bandstructure and low-energy approximation

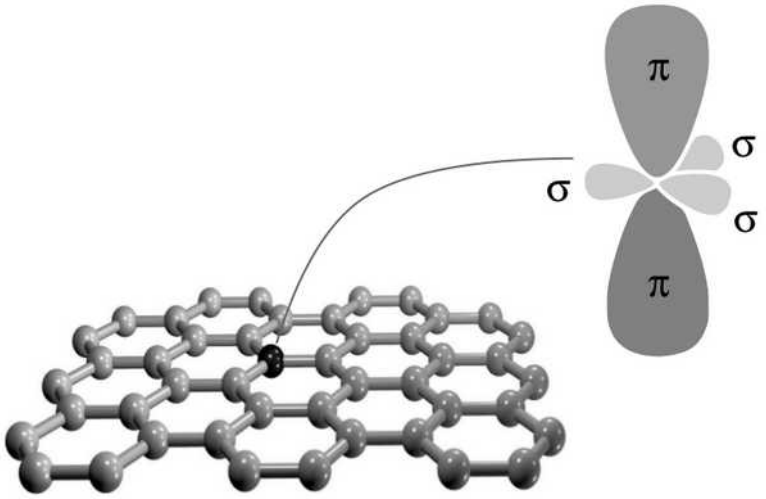

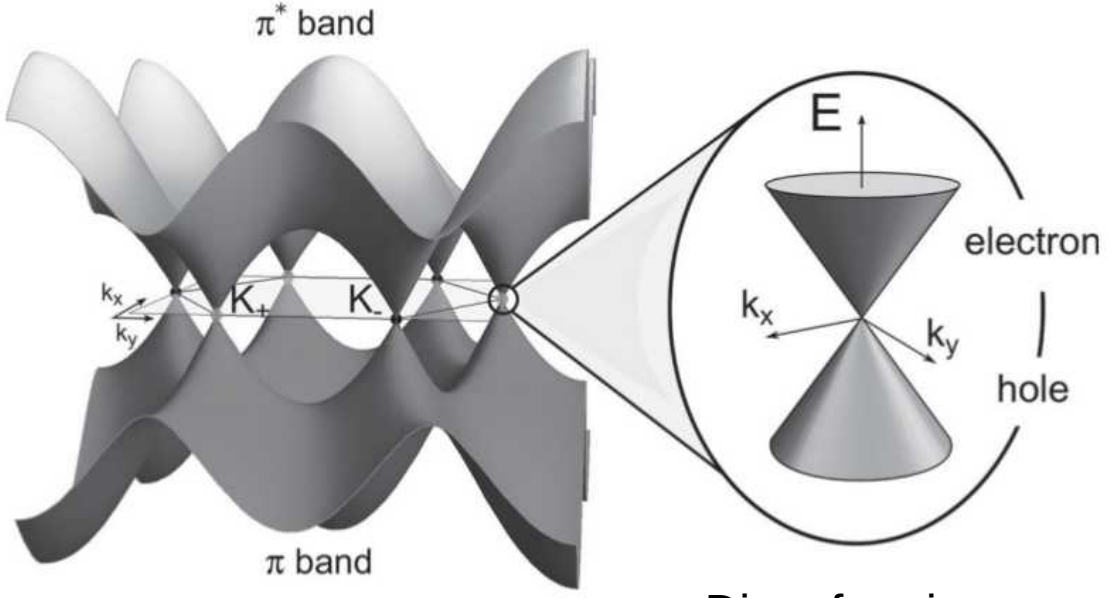

Dirac fermions

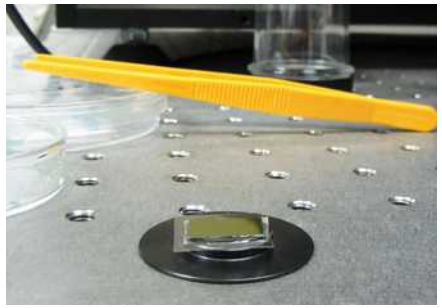

"CERN on a Desk"
A. Geim

$$\mathcal{H}_{K_+} = \hbar v_F \begin{pmatrix} 0 & k_x - ik_y \\ k_x + ik_y & 0 \end{pmatrix}$$

$$= v_F(p_x\sigma_x + p_y\sigma_y),$$

$$\hat{\sigma} = (\sigma_x, \sigma_y, \sigma_z) \qquad \mathcal{H}_{K_+} = v_F\hat{\sigma}.\mathbf{p},$$

Chirality and pseudospin

Chirality and pseudospin

An object that cannot be superimposed on its mirror image is called chiral

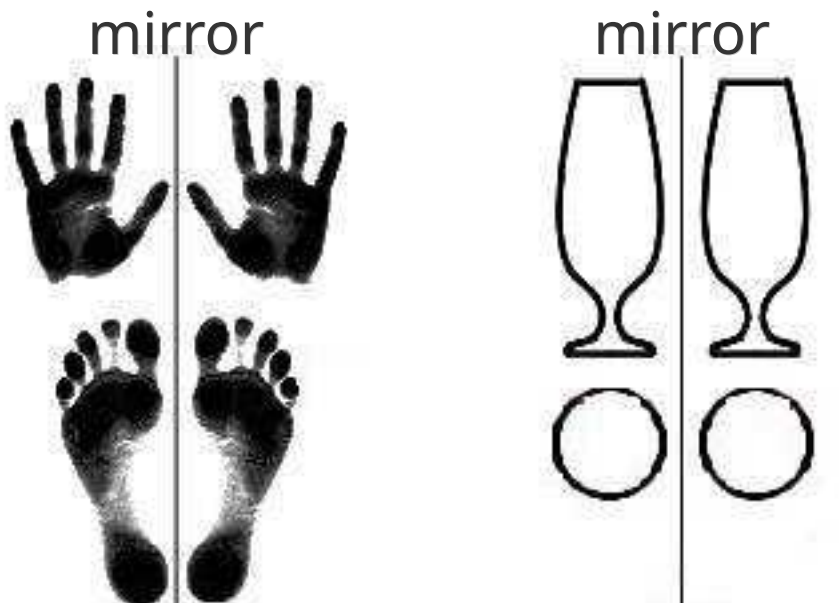

chiral objects

non-chiral objects

Chirality and pseudospin

The low-energy Hamiltonians around each valley are not the same, they are transposed (TRS).

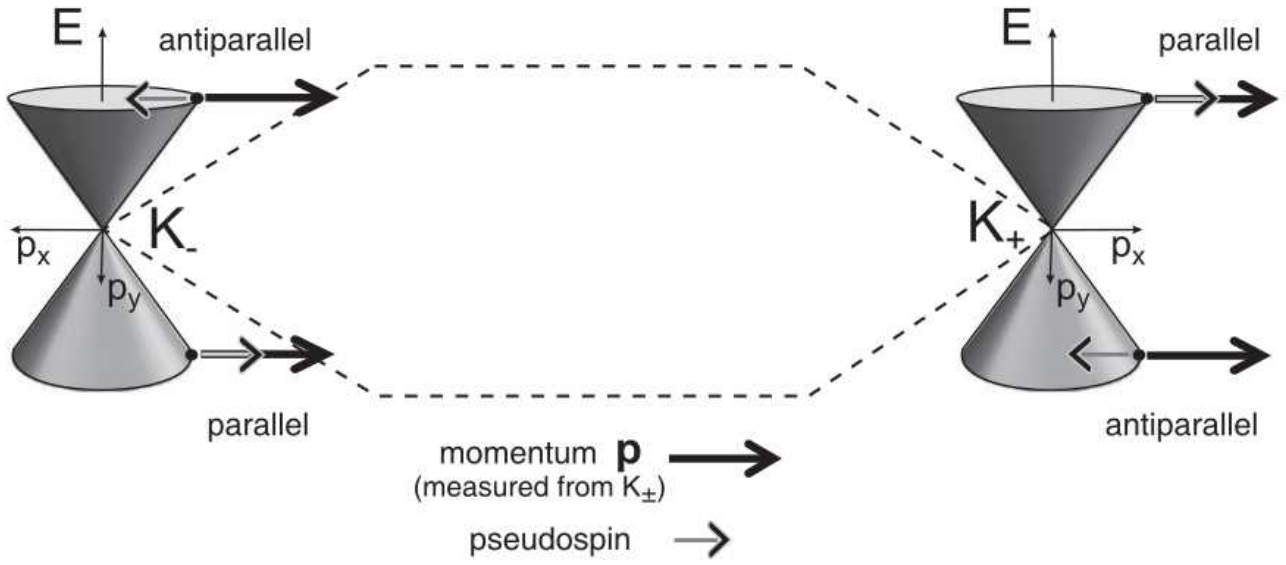

E>0

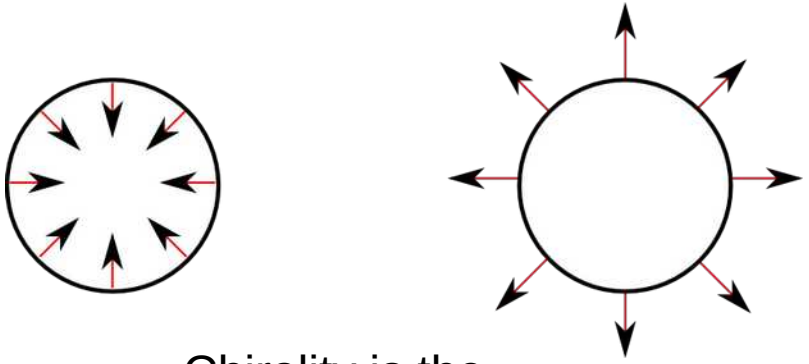

Chirality is the

See Exercise 2.13 (
onlin

Klein tunneling

(absence of backscattering)

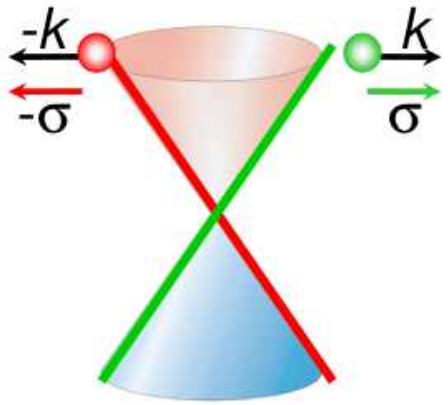

pseudospin

Electrons moving to the right $\rightarrow \sigma$

Electrons moving to the left $\leftarrow -\sigma$

T. Ando, J. Phys. Soc. Jpn. **67**, 857 (1998) [nanotubes]

Klein tunneling

(absence of backscattering)

Scattering backwards would require changing (“flipping”) the pseudospin
→ Absence of backscattering!

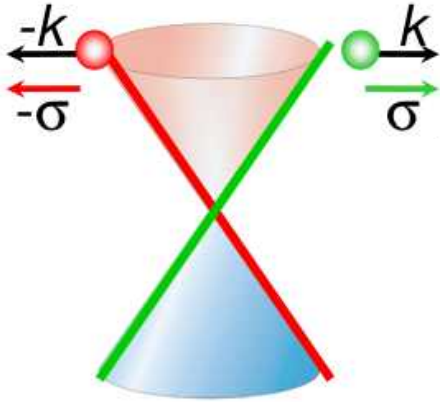

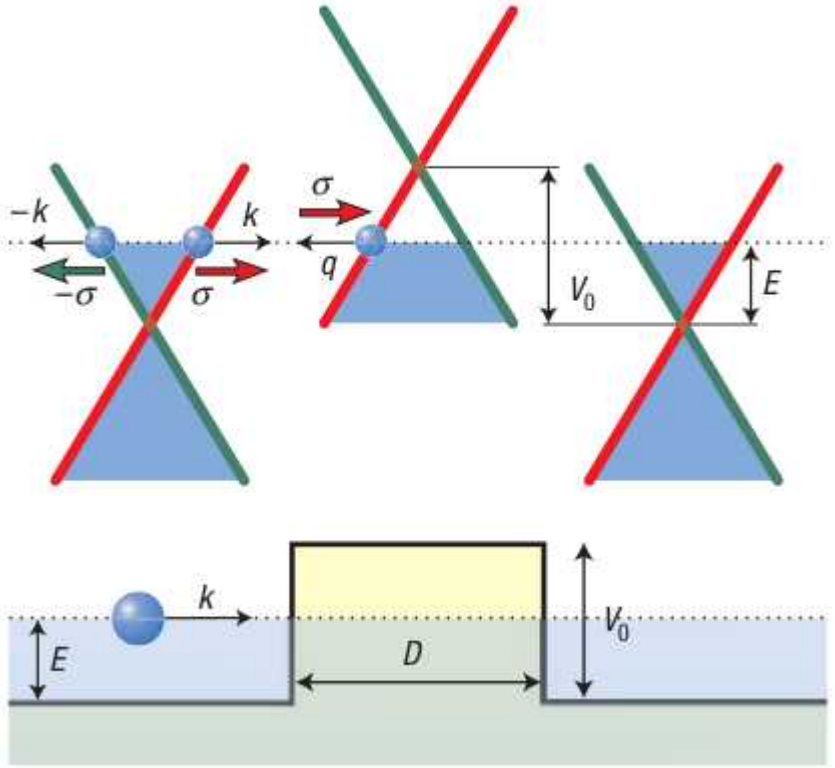

T. Ando, J. Phys. Soc. Jpn. **67**, 857 (1998) [nanotubes]

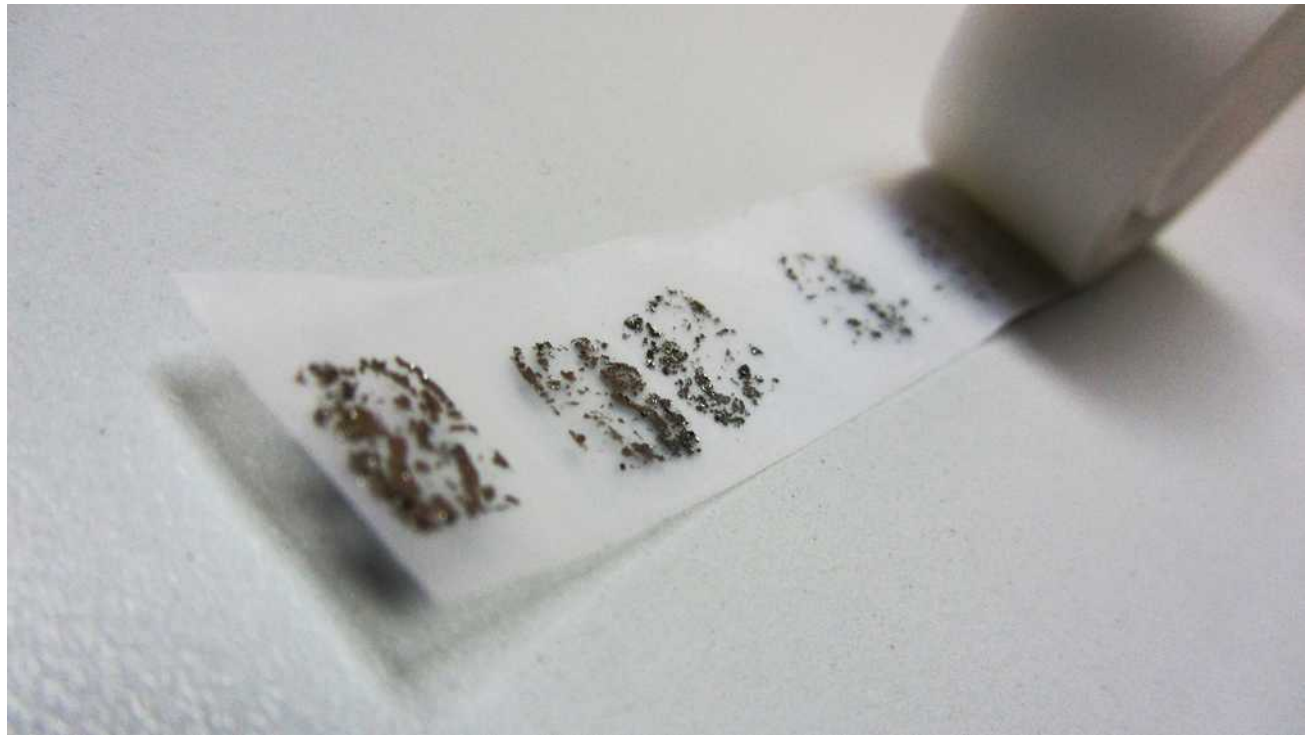

All the material from these lectures will be here: